Human umbilical cord mesenchymal stem cell-derived exosomes improve ovarian function in natural aging by inhibiting apoptosis

ZHONGKANG LI[1*], YIBIN LIU[1*], YANPENG TIAN[1,2], QIAN LI[1], WENXIN SHI[1], JINGKUN ZHANG[1], HUIHUI ZHANG[3], YI TAN[3,4], SHUANGSHUANG YANG[3], TAO YANG[5], XIANGHUA HUANG[1] and YANFANG DU[1]

[1]Department of Obstetrics and Gynecology, The Second Hospital of Hebei Medical University, Shijiazhuang, Hebei 050000; [2]Department of Obstetrics and Gynecology, The First Affiliated Hospital of Zhengzhou University, Zhengzhou, Henan 450052; [3]R&D Department, Shandong Qilu Cell Therapy Engineering Technology Co., Ltd.; [4]Institute of Immunotherapy, Shandong Yinfeng Life Science Research Institute, Jinan, Shandong 25000; [5]Department of Surgery, The Second Hospital of Hebei Medical University, Shijiazhuang, Hebei 050000, P.R. China

Received March 14, 2023; Accepted August 7, 2023

DOI: 10.3892/ijmm.2023.5297

Abstract. Prolonging the reproductive lifespan is beneficial for preserving the physical and psychological health of women. The transplantation of mesenchymal stem cell (MSC)-derived exosomes (MSC-Exos) has been reported to be a promising regenerative therapeutic strategy for restoring the function of aging ovaries. The present study thus evaluated the therapeutic efficacy of exosomes derived from human umbilical cord-MSCs (hUCMSC-Exos) in a mouse model of natural ovarian aging (NOA), and further investigated the role of exosomal microRNAs (miRNAs/miRs) in the mechanisms of this creative therapy. Specifically, following the administration of hUCMSC-Exos in mice with NOA, ovarian function was found to improve, as indicated by the restoration of follicle numbers and hormone levels. These exosomes were found to exhibit the ability to inhibit PTEN expression and suppress apoptosis both *in vivo* and *in vitro*. Subsequently, miRNA sequencing of the exosomes was performed, following which bioinformatics analysis was used to identify the highly expressed miRNAs that are capable of targeting PTEN expression. Through high-throughput sequencing and molecular analyses, miR-21-5p was found to be the highest in ranking in terms of expression, suggesting that hUCMSC-Exos can preserve ovarian function by suppressing PTEN expression to inhibit apoptosis by delivering miR-21-5p. On the whole, the results of the present study suggest that the application of exosomes can be used to restore ovarian function in mice with NOA. These positive findings also suggest that the transplantation of exosomes derived from MSCs holds promise as an agent against ovarian aging.

Correspondence to: Professor Yanfang Du or Professor Xianghua Huang, Department of Obstetrics and Gynecology, The Second Hospital of Hebei Medical University, 215 Heping West Road, Shijiazhuang, Hebei 050000, P.R. China
E-mail: duyanfang1973@163.com
E-mail: huangxh2003@163.com

*Contributed equally

Key words: natural ovarian aging, exosome, human umbilical cord mesenchymal stem cells, PTEN, miR-21-5p, apoptosis, proliferation

Introduction

The ovary plays a crucial role as a manager and regulator of various female physiological processes associated with female fertility, including ovulation and sexual hormone secretion (1). However, the process of aging indisputably has indisputable detrimental effects on ovarian function (2). Natural ovarian aging (NOA) is a degenerative condition that is characterized by the gradual decline in ovarian function, a process that is influenced by both genetics and environmental factors (3). The progressive loss of follicles and oocytes in terms of both quantity and quality as a result of aging has been reported to be strongly associated with significant ovarian dysfunction (4). When this progression is accelerated or advanced, it can lead to premature insufficiency and insufficient reserve of the ovary, resulting in pathological damage in females (5). In particular, decreased ovarian reserve can adversely affect the function of other organs and tissues, which contribute to reproductive senescence, urogenital symptoms, decreased bone density and cardiovascular disease (6). NOA is a physiological phenomenon which may cause organ dysfunctions and psychological burdens. Given the marked increase in the global average life expectancy, there has been a notable rise in the proportion of postmenopausal women (7). With improving living standards and increased health awareness, there are currently aspirations to either attenuate or partially reverse the process of NOA to enhance the quality of life. In 2015, a study published in 'Nature' emphasized the importance of addressing aging seriously, as it serves as a catalyst for a long list of diseases in the human body (8). Therefore, the challenge lies in effectively addressing the natural aging process in the ovary within the field of medicine.

Hormone replacement therapy has traditionally been applied for addressing menopausal symptoms. However, its

non-fundamental reconstruction of the ovary and associated side-effects always result in unsatisfactory efficiency (9). Therefore, there is an urgent demand for a novel therapeutic approach that can fundamentally improve ovarian function in the management of NOA. With the increasing utilization of regenerative therapy in medicine, mesenchymal stem cells (MSCs) and MSC-derived exosomes (MSCs-Exos) have emerged as a potential means to achieve such a restoration of ovarian function (10). MSCs possess various characteristics, including low immunogenicity, and paracrine and multi-directional differentiation capabilities, enabling them to reconstruct damaged tissues and organs (11). In particular, human umbilical cord-derived MSCs (hUCMSCs) can be easily isolated and have high proliferative capacities (12), leading to their commercialization by biotechnology companies and widespread application in basic research, biomedical applications, clinical trials or even medical therapies (13-15). The paracrine effectors of MSCs, namely their secretome, have been reported to exert long-term therapeutic effects by transporting microRNAs (miRNAs/miRs) and proteins (cytokines or growth factors) to target recipient cells in injured organs (16,17). Exosomes are major mediators of the paracrine function of MSCs by facilitating intercellular communications by delivering a variety of biomolecules (18). With an average diameter of 100 nm, these exosomes possess the ability to regulate gene expression through the miRNAs being transported (19).

Follicular atresia and functional failure are prominent pathological features of NOA (20). Previous research has demonstrated that the apoptosis of granulosa cells (GCs) within follicles serves as the main underlying cause of follicle impairment (21). During follicular atresia, there is an elevation in the expression level of apoptosis-associated genes, a downregulation in that of anti-apoptotic genes and an increase in the activity of the caspase family of proteins within GCs (22,23). Therefore, modulating he expression of apoptotic genes to inhibit GC apoptosis represents a promising strategy for alleviating the progression of NOA. PTEN has previously been documented to be an important regulator of various physiological processes, including proliferation, migration and apoptosis (24). The involvement of PTEN in the regulation of apoptosis is particularly well-documented, since it inhibits AKT activation, a critical suppressor of apoptosis (25). In addition, the PTEN/PI3K/AKT signaling pathway plays a crucial role in governing the recruitment and growth of primordial follicles (26), where PTEN plays a key role in the regulation of follicle activation. Previous research has reported that the inhibition of PTEN expression can promote follicle activation and restore reproductive function (27). During exosome transplantation, MSC-Exos can carry miRNAs that have the ability to target and inhibit PTEN expression, thereby reducing cellular apoptosis and restoring the functionality of target organs. A previous study found that miR-144 derived from MSC-Exos blocked cardiomyocyte apoptosis by targeting PTEN and modulating the AKT pathway (28). Although previous studies have demonstrated the potential of MSC-Exos in improving ovarian function in cases of premature ovarian insufficiency (10,29), limited attention has been paid to the detection of the effects of MSCs or MSC-Exos on NOA (30). Furthermore, the underlying mechanisms through which exosomal miRNAs can alleviate ovarian cells apoptosis in NOA remains poorly understood.

Therefore, the primary aim of the present study was to evaluate the potential of hUCMSC-derived exosomes (hUCMSC-Exos) in restoring ovarian function in a mouse model of NOA and to explore the regulatory effects of exosomes on PTEN expression and apoptosis both *in vivo* and *in vitro*. In addition, the high-throughput sequencing of exosomes was conducted to identify highly expressed miRNAs that can target PTEN expression, following which their effects on GC apoptosis were validated. It is hoped that the findings of the present study will lay the foundation for future investigations of hUCMSC-Exos for countering ovarian aging.

Materials and methods

Identification of hUCMSCs and exosomes. The hUCMSCs used herein were purchased from Shandong Qilu Cell Therapy Engineering Technology Co., Ltd. and cultured in a complete medium at 37˚C with 5% CO_2. The identification of hUCMSCs was performed by following a previously established protocol (31). Initially, their morphology was confirmed using a light microscope (Carl Zeiss AG). Subsequently, the osteogenesis differentiation kit (A1007201, Gibco; Thermo Fisher Scientific, Inc.) and adipogenesis differentiation kit (A1007001, Gibco; Thermo Fisher Scientific, Inc.) were utilized for the induction of the differentiation of the MSCs. Alizarin Red staining and Oil Red O staining were performed on the cells following the induction of cell differentiation. For Alizarin Red staining, the cells were fixed using 4% paraformaldehyde at room temperature for 10-20 min. A staining solution of 0.1% Alizarin Red in Tris-HCl buffer at pH 4.2 (MilliporeSigma) was applied to the cells for 20-30 min at room temperature. Following staining, the cells were rinsed with distilled water until color fading ceased. Similarly, for Oil Red O staining, the cells were fixed with 4% paraformaldehyde at room temperature for 10-20 min. A 0.5% Oil Red O staining solution in isopropanol (MilliporeSigma) was applied to the cells for 15-20 min at room temperature. Subsequently, the cells were washed with 70% ethanol until color fading ceased. Staining results were observed and documented under a microscope (Axio Imager.D2; Carl Zeiss AG). Finally, flow cytometry (BD FACSCanto II; BD Biosciences) was utilized to detect the expression of positive surface markers (CD44, CD73, CD90, and CD105; Biolegend, Inc.) and negative surface markers (CD34, CD45, and HLA-DR; Biolegend, Inc.) of MSCs.

The extraction of exosomes was successfully performed following a previously established method (32). Subsequently, the identification of exosomes was performed in accordance with the standards set by the International Society for Extracellular Vesicles (33). The size distribution and concentration of exosomes were determined using the Flow Nano Analyzer (Particle Metrix GmbH). Additionally, the morphologies of the exosomes were observed using a transmission electron microscope (Thermo Fisher Scientific, Inc.). Lastly, the surface markers of exosomes (CD9, CD63, and CD81; Biolegend, Inc.) were detected using flow cytometry (BD Biosciences).

Single-cell RNA-seq (scRNA-seq) analysis of aging primate ovaries. Bioinformatics analysis was performed to investigate the expression levels of PTEN and apoptosis-related genes in aging primate ovaries using single-cell data. The scRNA-seq data from the GSE130664 dataset (34) were obtained from the Gene Expression Omnibus (GEO) database (https://www.ncbi.nlm.nih.gov/geo/). This dataset was derived from 2,601 single cells with high-quality transcriptomes collected from the ovaries of 4 young and 4 aged monkeys for scRNA-seq analysis (34). The 'Seurat' R package was utilized for quality control, normalization, dimensional reduction and processing of the scRNA-seq expression data. Genes expressed in fewer than three cells were excluded, whereas cells with <50 genes were removed from the analysis. The expression data were then normalized, dimensionally reduced and clustered using the t-distributed stochastic neighbor embedding (t-SNE) method. Cluster annotation was performed using cell markers from the 'CellMarker' database (35) and from a previous study (34). Finally, the expression of PTEN and apoptosis-related molecules was presented.

Experimental animals and treatment with hUCMSC-Exos. A total of 36 female C57BL/6 mice, aged 3 months (n=12) and 14 months (n=24), were obtained from SPF Biotechnology (Beijing, China). The principles outlined in the Declaration of Helsinki and the Guidelines for the Care and Use of Laboratory Animals of the Chinese Institute of Health were strictly adhered to in the present study. The authors also complied with the ARRIVE guidelines. Ethical approval for the animal experiments was obtained from the Ethical Committee of Second Hospital of Hebei Medical University (approval no. 2021-AE034). All animal experiments conducted in the present study followed the guidelines and regulations specified in this ethical approval. The aging mice were equally and randomly divided into two groups as follows: the NOA group and Exos group (n=12 per group). Additionally, a group of 3-month-old mice, referred to as the Young group (n=12), was also included in the present study. The animals were kept in individually ventilated cages with autoclaved aspen woodchips and a mouse house, a maintaining a temperature of 21±2˚C, a 12:12-h light-dark cycle, and a relative humidity of 55±10%. They were provided with unrestricted access to a commercially prepared autoclaved dry rodent diet and water. The health of the animals was monitored on a daily basis through routine visual checks. In the animal experiments, humane endpoints were established to ensure the welfare of the animals and to minimize suffering. The humane endpoints included the following: A 20% decrease in body weight compared to the pre-study weight; continuous 4-day anorexia with significant weight loss; persistent diarrhea or vomiting with no response to treatment; conditions unresponsive to clinical treatments, such as organ failure, respiratory distress and sepsis; severe hypothermia or hyperthermia unresponsive to corrective measures; severe complications resulting from medical/surgical interventions or other experimental manipulations with no available corrective measures; severe self-injurious behaviors unmanageable by behavioral interventions, medical treatments, and/or research removal. These humane endpoints were implemented in accordance with the guidelines and regulations of the authors' institution to ensure the ethical conduct of the research. Following the adaptive feeding period, the mice in the Exos group received intraperitoneal injections of 150 μg exosomes twice, with a 7-day interval between injections, based on observations from a previous study (32). By contrast, mice in the NOA group were injected with an equivalent volume of phosphate-buffered saline (PBS; Wuhan Servicebio Technology Co., Ltd.), whilst the mice in the Young group did not receive any therapeutic interventions. No mice were found dead prior to euthanasia. At 2 weeks after the injection of the exosomes (36), the animals were euthanized by an intraperitoneal injection of an overdose of pentobarbital (100 mg/kg) in all three groups (n=36). The confirmation of animal death was determined by examining whether the heartbeat of the animal had ceased completely and whether the pupils were dilated. Ovarian tissue and serum samples were then collected for subsequent experimental analyses. Each data analysis included at least three replicate molecular experiments, with a minimum of six animal samples per group in each experiment.

Culture and identification of human GCs. The human ovarian granulosa cell line, HO-23 (37,38), was obtained from Qingqi (Shanghai) Biotechnology Development Co., Ltd. (cat. no. BFN60808800) and cultured in DMEM (Gibco; Thermo Fisher Scientific, Inc.) supplemented with 10% exosome-depleted FBS (Gibco; Thermo Fisher Scientific, Inc.) at 37˚C and 5% CO_2.

The immunofluorescence staining of follicle-stimulating hormone (FSH) receptor (FSHR) was performed to identify the human GCs (hGCs), as FSHR is specifically expressed in the cytoplasm of ovarian GCs. Initially, the complete medium was removed, and the cells were washed three times with PBS (Wuhan Servicebio Technology Co., Ltd.). Subsequently, permeabilization was achieved using 0.3% Triton X-100 (Wuhan Servicebio Technology Co., Ltd.), followed by blocking with 5% goat serum (Wuhan Servicebio Technology Co., Ltd.). The cells were then incubated overnight at 4˚C with primary antibody against FSHR (1:800; cat. no. GB11275-1-100, Wuhan Servicebio Technology Co., Ltd.). On the following day, the cells were incubated with a FITC-conjugated secondary antibody (1:400; cat. no. GB22303, Wuhan Servicebio Technology Co., Ltd.) for 1 h. Finally, the cell nuclei were stained with DAPI for 10 min at room temperature (cat. No.: 0100-20, SouthernBiotech). Images were captured using a ZEISS fluorescence microscope (Carl Zeiss AG).

Western blot analysis. Western blot analyses were performed to examine protein expression in ovarian tissues and GCs. The samples were first lysed using RIPA lysis buffer (Wuhan Servicebio Technology Co., Ltd.). The protein concentrations were measured using the BCA protein assay kit (Beijing Solarbio Science & Technology Co., Ltd.), before the protein samples were denatured at 100˚C for 10 min. Subsequently, the proteins were separated in SDS-PAGE (10%) and transferred onto PVDF membranes. In the adjacent lanes of the target samples, a protein molecular weight marker was utilized. To conserve the usage of antibodies, we subjected the membrane to precise trimming based on the protein quantity of the target molecule, resulting in a final presentation of the membrane in a strip-like format. These membranes were then blocked with

Table I. Primer sequences used for RT-qPCR.

Gene	Forward primer	Reverse primer
Human PTEN	5'- TTTGAAGACCATAACCCACCAC-3'	5'-ATTACACCAGTTCGTCCCTTTC-3'
Human Bax	5'-CCCGAGAGGTCTTTTTCCGAG-3'	5'-CCAGCCCATGATGGTTCTGAT-3'
Human Bcl-2	5'-GGTGGGGTCATGTGTGTGG-3'	5'-CGGTTCAGGTACTCAGTCATCC-3'
Human caspase-3	5'-CATGGAAGCGAATCAATGGACT-3'	5'-CTGTACCAGACCGAGATGTCA-3'
Human caspase-9	5'-CTCAGACCAGAGATTCGCAAAC-3'	5'-GCATTTCCCCTCAAACTCTCAA-3'
Human GAPDH	5'-ACAACTTTGGTATCGTGGAAGG-3'	5'-GCCATCACGCCACAGTTTC-3'
MousePTEN	5'-CACACTGTTCCTCGTTATGAAGA-3'	5'-CTTGAGATCCCGATGGGCAAT-3'
Mouse Bax	5'-TGAAGACAGGGGCCTTTTTG-3'	5'-AATTCGCCGGAGACACTCG-3'
Mouse Bcl-2	5'-GCTACCGTCGTGACTTCGC-3'	5'-CCCCACCGAACTCAAAGAAGG-3'
Mouse caspase-3	5'-CTGACTGGAAAGCCGAAACTC-3'	5'-CGACCCGTCCTTTGAATTTCT-3'
Mouse caspase-9	5'-TCCTGGTACATCGAGACCTTG-3'	5'-AAGTCCCTTTCGCAGAAACAG-3'
Mouse GAPDH	5'-AGGTCGGTGTGAACGGATTTG-3'	5'-GGGGTCGTTGATGGCAACA-3'
Human miR-21-5p	5'-ACACTCCAGCTGGGTAGCTTATCAGACTGA-3'	5'-ATGGTGTCGTGGAGTCG-3'
Human miR-26a-5p	5'-ACACTCCAGCTGGGTTCAAGTAATCCAGGA-3'	5'-ATGGTGTCGTGGAGTCG-3'
U6	5'-CTCGCTTCGGCAGCACA-3	5'-AACGCTTCACGAATTTGCGT-3'

5% skimmed milk for 2 h and incubated overnight at 4˚C with primary antibodies against PTEN (1:1,000; cat. no. bs-0748R, BIOSS), Bax (1:500; cat. no. AF1270, Beyotime Institute of Biotechnology), Bcl-2 (1:500; cat. no. bs-4563R, BIOSS), caspase-3 (1:500; cat. no. AF1213, Beyotime Institute of Biotechnology), caspase-9 (1:1,000; cat. no. AF1264, Beyotime Institute of Biotechnology) or GAPDH (1:2,000; cat. no. GB11002-100, Wuhan Servicebio Technology Co., Ltd.). The membranes were cut prior to antibody hybridization, resulting in the absence of the full-length blot. On the following day, the membranes were incubated with an HRP-conjugated secondary antibody (1:5,000, cat. no. GB23303, Wuhan Servicebio Technology Co., Ltd.) for 1 h. After washing the membranes with PBS-Tween-20, the protein levels were quantified using the ChemiDoc MP Imaging System (Bio-Rad Laboratories, Inc.). For the statistical analysis of the western blot data using Image Lab™ software (version 6.0, Bio-Rad Laboratories, Inc.), at least three replicate experiments were performed, with each experiment including at least six animal samples per group.

Reverse transcription-quantitative PCR (RT-qPCR). Initially, total RNA was extracted using TRIzol® reagent (Invitrogen; Thermo Fisher Scientific, Inc.). The MonScript™ RTIII All-in-One Mix with dsDNase (Monad Biotech Co., Ltd.) was used for the reverse transcription of total RNA into cDNA. To perform qPCR, specific primers were obtained from the primer bank and synthesized by Sangon Biotech Co., Ltd. The primer sequences are presented in Table I. GoTaq® qPCR Master Mix (Promega Corporation) was used for qPCR with the Bio-Rad CFX96 detection system, using the thermocycling conditions of 95˚C for 10 min, followed by 40 cycles of 95˚C for 15 sec and 60˚C for 60 sec. The relative expression of miRNA and mRNA was calculated using the $2^{-\Delta\Delta Cq}$ method (39). To ensure robust statistical analysis of the RT-qPCR data, a minimum of three independent replicate experiments were performed. Each experiment consisted of at least six animal samples per group.

TUNEL assay. TUNEL assays on the ovarian sections and hGCs were conducted to assess the level of apoptosis. The procedure involved permeabilization using 0.3% Triton X-100 (Beijing Solarbio Science & Technology Co., Ltd.) and incubation with the TUNEL detection solution (Beyotime Institute of Biotechnology) for both the ovarian sections and GCs. The nuclei were subsequently labeled with the DAPI solution (SouthernBiotech) at room temperature. The staining results were observed under a fluorescence microscope (Carl Zeiss AG), where the apoptotic cell nuclei appeared green.

5-Ethynyl-2'-deoxyuridine (EdU) assay. EdU assay was used to estimate the extent of proliferation in ovarian tissues and hGCs. EdU is a marker of DNA synthesis that can be administered to animals through injection or feeding (40). In the present study, EdU was dissolved in PBS at a concentration of 50 mg/kg and intraperitoneally injected into the mice. After 4 h, the mice were rapidly sacrificed (the euthanasia method was the same as the method described above) and their ovaries were collected. Paraffin-embedded sections of the ovarian tissues were prepared using standard procedure (41). Permeabilization of these slides was achieved using 0.3% Triton X-100. After being washed with PBS, the slides were stained with reaction solution (Beyotime Institute of Biotechnology). Cell nuclei were labeled with Hoechst 33342 at room temperature (1:1,000; Beyotime Institute of Biotechnology). The slides were observed using a fluorescence microscope (Carl Zeiss AG), before the presence of EdU was visualized as a fluorescence signal.

For the EdU assay of the cells, cells in the logarithmic growth phase were seeded in a six-well plate, treated with 10 μM EdU (ST067, Beyotime Institute of Biotechnology) and incubated for 2 h at 37˚C. The cells were then fixed with 4% paraformaldehyde for 30 min at room temperature. Permeabilization was achieved using 0.3% TritonX-100 and the cells were stained with EdU reaction solution at room temperature (C0071S, Beyotime Institute of Biotechnology).

Similarly, nuclei were labeled with Hoechst 33342 (Beyotime Institute of Biotechnology). After completing these steps, images were captured using a fluorescence microscope (Carl Zeiss AG).

Tracing experiment of exosomes in vivo. To investigate the uptake and migration of the transplanted hUCMSC-Exos in the ovaries of mice, the exosomes were labeled with 5 μl/Test EvLINK 555 (cat. no. CL012100220; Tingoscience) and incubated at room temperature for 30 min. The labeled exosomes were then centrifuged at 10,000 x g for 15 min at 4˚C, which was then repeated five times to remove free fluorescent probes and small molecules. Subsequently, the labeled exosomes were purified using a CORE400 column (Tianyan Biotech Co., Ltd.) (http://cesi.sinopae.com/index.html) in pH 7.4 buffer, before the mice were injected with these purified labeled exosomes. In total, 5 days later, the ovarian tissues of mice were obtained for frozen sections. The cell nuclei were labeled with DAPI at room temperature and images were captured using a fluorescence microscope (AxioCam HRc; Carl Zeiss AG).

Ovarian morphology and follicle counts. The ovarian tissues were obtained from the euthanized mice following the completion of the exosome-mediated therapy. These tissues were fixed in 4% paraformaldehyde for over 48 h at room temperature. Following the completion of paraffin-embedding, the ovarian tissues were sliced into 5-μm-thick sections. From each group, 6 mice were randomly selected and their ovaries were consecutively sectioned. For hematoxylin and eosin (H&E) (MilliporeSigma) staining, the 10th slice of all ovaries was selected. During the hematoxylin staining step, the tissues are exposed to the stain at room temperature for approximately 5-10 min, allowing for the visualization of cell nuclei. Conversely, in the subsequent eosin staining step, the tissues are subjected to the stain at room temperature for 1-3 min, providing coloration to cytoplasmic components and extracellular matrix. Additionally, three sections at 200-μm intervals with the largest cross-sectional area were selected to count the number of follicles at each stage. Ovarian morphology was observed using a light microscope (Carl Zeiss AG) and all types of follicles were counted. The average number of follicles at each stage was calculated. The stage of individual follicles was determined using the following criteria: i) The primordial follicle has an oocyte surrounded by a layer of flat squamous GCs; ii) the primary follicle has an oocyte surrounded by a single layer of cuboidal GCs; iii) the secondary follicle has an oocyte surrounded by more than one layer of cuboidal GCs without a visible antrum; iv) the mature follicle exhibits a large antral space, prominent cumulus and a visible oocyte crown; and v) the atretic follicle has a collapsed follicular wall, a disappearance of oocyte structure and shrinkage of the zona pellucida.

ELISA. The blood from sacrificed mice was collected and the serum was obtained by centrifugation of the blood at 5,000 rpm for 10 min at 4˚C. The levels of anti-Müllerian hormone (AMH), estradiol (E_2) and FSH in serum were measured using ELISA Kits (cat. nos. 15775, 1609 and 23789 Meimian Technology Co., Ltd.) according to the manufacturer's instructions. Briefly, 50 μl serum from each mouse were added to the coated wells for incubation at 37˚C for 30 min. After washing the wells five times, HRP-conjugated antibodies were added. Following another round of washing, color development solution was added and incubated with the wells at 37˚C for 30 min. Finally, the reaction was terminated using stop buffer and the optical density was measured at a wavelength of 450 nm using a microplate reader (BioTek Epoch; BioTek Instruments, Inc.). The concentrations of these hormones were determined by comparing the readings to the standard curve. For statistical analysis of the ELISA results, a minimum of three replicate experiments were conducted, with each experiment including at least six animal samples per group.

Immunofluorescence staining. Firstly, the paraffin-embedded ovarian sections (5-μm-thick) underwent antigen retrieval using sodium citrate buffer (Wuhan Servicebio Technology Co., Ltd.). Subsequently, permeabilization was performed using 0.3% Triton X-100 (Beijing Solarbio Science & Technology Co., Ltd.) and blocking was performed with 5% goat serum (Wuhan Servicebio Technology Co., Ltd.). The slides were then incubated overnight at 4˚C with primary antibodies, including Ki67 (1:600; cat. no. GB111141-100, Wuhan Servicebio Technology Co., Ltd.) and proliferating cell nuclear antigen (PCNA; 1:600; cat. no. GB11010-100, Wuhan Servicebio Technology Co., Ltd.). The following day, the slides were incubated with the secondary FITC-conjugated antibody (1:400; cat. no. GB22303, Wuhan Servicebio Technology Co., Ltd.) and Cy3-conjugated antibody (1:400; cat. no. GB21303, Wuhan Servicebio Technology Co., Ltd.) for 1 h. Finally, the cell nuclei were stained with DAPI for 10 min at room temperature (SouthernBiotech), and the slides were observed under a fluorescence microscope (Carl Zeiss AG).

Immunohistochemistry. The ovarian tissue sections underwent the same procedures in terms of antigen retrieval, permeabilization and blocking as those for immunofluorescence staining. Subsequently, primary antibodies (Ki67, 1:800; cat. no. GB111141-100, Wuhan Servicebio Technology Co., Ltd.) were incubated with the ovarian tissue sections at 4˚C overnight. The following day, the biotinylated secondary antibodies (1:2,000; cat. no. GB21303GB23303, Wuhan Servicebio Technology Co., Ltd.) were applied to the slides and incubated at room temperature for 1 h. Finally, the slides were stained using a reaction solution containing diaminobenzidine (ZSGB-BIO). ImageJ software (version 1.53, National Institutes of Health;) was utilized to analyze the immunofluorescence staining and the relative density was measured by normalizing the fluorescence intensity to the Young group.

Transfection with miR-21-5p inhibitor/mimics. To perform transfection with miR-21-5p inhibitor/mimics, RNA oligos were obtained from the Genepharma Co., Ltd. The sequences are presented in Table II. A total of 100 μl serum-free Opti-MEM was utilized to dilute 5 μl Lipofectamine™ 2000® (cat. no. 11668019, Thermo Fisher Scientific, Inc.), 50 nmol miR-negative control (NC) and 50 nmol miR-21-5p mimics and inhibitors separately. Following a 5-min incubation at room temperature, Lipofectamine™ 2000 was mixed with either miR-NC or miR-21-5p mimics/inhibitor, before the resulting mixture was then incubated for 20 min at room

Table II. Sequences for miRNA mimics and inhibitors.

Gene	Sequences
hsa-miR-21-5p mimics	Sense: 5'-UAGCUUAUCAGACUGAUGUUGA-3'
	Antisense: 5'-AACAUCAGUCUGAUAAGCUAUU-3'
Mimics negative control	Sense: 5'-UUCUCCGAACGUGUCACGUTT-3'
	Antisense: 5'-ACGUGACACGUUCGGAGAATT-3
hsa-miR-21-5p inhibitor	5'-UCAACAUCAGUCUGAUAAGCUA-3'
Inhibitor negative control	5'-CAGUACUUUUGUGUAGUACAA-3'

temperature. Subsequently, all these reagents were added to the cell medium for incubation for 6 h at 37˚C. The cells were collected at 2 days following transfection for use in subsequent experiments.

Establishment of cell apoptosis model. To investigate the effects of hUCMSC-Exos on GCs apoptosis, a series of cell-related mechanistic studies were performed. The cells were divided into three groups for experimentation. In the cyclophosphamide (CTX) group, hGCs were co-cultured with 30 μM CTX (Sigma-Aldrich; Merck KGaA) for 24 h. In the Exos group, after the CTX intervention, 30 μg/ml exosomes were added to the medium of hGCs. In the normal group, which served as the control, the GCs were cultured in the ordinary cellular medium without any additional interventions.

To assess the function of miR-21-5p in exosome-mediated therapy, miRNA inhibitor and mimics transfection experiments were performed. For the miRNA inhibitor test, the experiments were divided into four groups based on the different interventions: The CTX group involved hGCs treated with CTX without exosomes administration; in the Exos group, CTX-treated hGCs were co-incubated with hUCMSC-Exos; in the Exos + miR-21-inhibitor group, CTX-treated hGCs were co-cultured with hUCMSC-Exos transfected with miR-21-inhibitor; in the Exos + miR-21-inhibitor NC group, which served as a control, hGCs were treated with hUCMSC-Exos transfected with a NC of the inhibitor. For miRNA mimics transfection, the cellular experiments were grouped similarly to those of the miRNA inhibitors, namely the CTX group, Exos + miR-21-mimics group, Exos + miR-21-mimics NC group and the Exos group. Exos + miR-21-mimics involved the transfection of miR-21 mimics and co-incubation with hUCMSC-Exos. In the Exos + miR-21-mimics NC group, mimics NC was transfected into the cell models.

Fluorescent imaging of exosome uptake. To assess the uptake of hUCMSC-Exos by hGCs, a labeling experiment was performed using Dil dye (Life Technologies; Thermo Fisher Scientific, Inc.). The hUCMSC-Exos were first labeled with Dil dye (10 μM) and then incubated with hGCs at 37˚C and 5% CO_2 for 24 h. Following incubation, the cells were washed to remove any non-internalized exosomes. Subsequently, the hGCs were stained with Calcein-AM (Life Life Technologies; Thermo Fisher Scientific, Inc.) for 30 min at 37˚C. Finally, a fluorescence microscope (AxioCam HRc; Carl Zeiss AG) was used to capture images of the labeled exosomes within the hGCs.

Cell Counting Kit-8 (CCK-8) assay. The proliferation of the hGCs was assessed using CCK-8 assay. After the medium of hGCs was replaced according to the aforementioned intervention methods, 10 μl CCK-8 solution (Wuhan Servicebio Technology Co., Ltd.) were added to each well and incubated with hGCs for 4 h at 37˚C. Subsequently, the absorbance of the medium at 450 nm was measured using a microplate reader (BioTek Epoch, BioTek Instruments, Inc.). This procedure was repeated on the following 5 days to evaluate the proliferative ability of the hGCs.

miRNA sequencing and bioinformatics analysis. The exosomal miRNAs derived from hUCMSCs were extracted and the quantity of miRNA was examined. For the preparation of small RNA sequencing libraries, the TruSeq Small RNA Sample Prep Kits (Illumina, Inc.) were employed. Once the library preparation was completed, the constructed library was subjected to sequencing using the Illumina Hiseq2000/2500 platform with a read length of 50 pb. Subsequently, the Kyoto Encyclopedia of Genes and Genomes (KEGG) analysis (42) was performed to highlight the pathways that were predominantly targeted by the exosomal-miRNAs.

Statistical analysis. The results of the present study are presented as the mean ± standard deviation (SD). Statistical analysis was performed using the SPSS 26.0 software (IBM, Corp.). Specifically, comparisons between two groups were conducted using a Student's t-test (unpaired), while one-way ANOVA was used for comparisons among multiple groups followed by Tukey's post hoc test. A P-value <0.05 was considered to indicate a statistically significant difference.

Results

Characterization of hUCMSCs and exosomes. The features of hUCMSCs and exosomes were identified in the present study. The morphology of the hUCMSCs was observed under a microscope' the cells exhibited a fibroblast-like morphology (Fig. 1A). The hUCMSCs were then cultured in conditioned medium, prior to induction with differentiation and were then assessed using Alizarin Red staining (which revealed calcium deposition) and Oil Red O staining (which revealed lipid vacuole accumulation) (Fig. 1B). These results indicated that *ex vivo* conditional culture systems can effectively induce hUCMSCs to

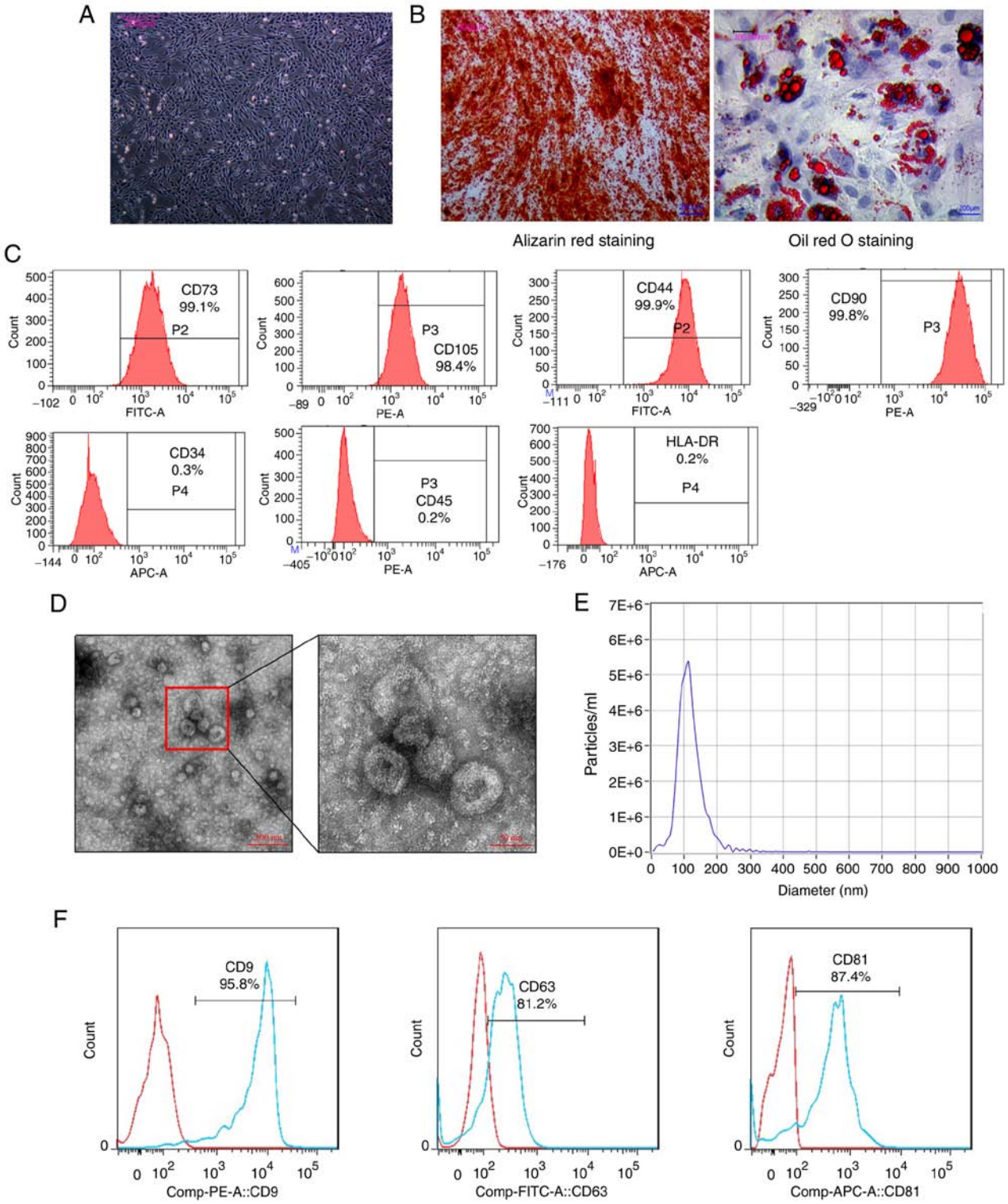

Figure 1. Characterization of hUCMSCs and hUCMSC-Exos. (A) Fibroblast-like morphology of hUCMSCs. Scale bar, 200 μm. (B) Osteogenic differentiation of hUCMSCs demonstrated by Alizarin Red staining and adipogenic differentiation of hUCMSCs demonstrated using Oil Red O staining. Scale bars, 200 μm. (C) Flow cytometric analysis confirming positive expression of CD44, CD73, CD90 and CD105 as surface markers of hUCMSCs, and the negative expression of CD34, CD45 and HLA-DR. (D) Cup-shaped morphology and distinct membrane structure of exosomes observed under a transmission electron microscope. Scale bar, 50 and 200 nm. (E) Size distribution and concentration analysis of exosomes showing a range of 30 to 150 nm in size and a high concentration. (F) Flow cytometry demonstrating the positive expression of CD9, CD63 and CD81 in hUCMSC-Exos. hUCMSCs, human umbilical cord-derived mesenchymal stem cells; hUCMSC-Exos, hUCMSC-derived exosomes.

differentiate into various cell types. The surface antigen expression profile of the hUCMSCs was then characterized using flow cytometry. The analysis revealed that the hUCMSCs were positive for CD73 (99.1%), CD105 (98.4%), CD44 (99.9%) and CD90 (99.8%) expression, while they were negative for CD34 (0.3%), CD45 (0.2%) and HLA-DR (0.2%) expression (Fig. 1C). These surface antigen characteristics align with those of the established criteria used for defining hUCMSCs.

In accordance with the identification criteria for extracellular vesicles, exosomes derived from the hUCMSCs were then characterized (33). Transmission electron microscopy revealed the cup-like morphology of the hUCMSC-Exos, displaying a distinctive membrane structure (Fig. 1D). Size distribution and concentration analysis demonstrated that the concentration of exosomes was $8.0x10^{10}$ particles/ml, where only extracellular vesicles within the diameter range of 30-150 nm were classified as exosomes (Fig. 1E). In addition, the exosomes stained positive for CD9, CD63 and CD81 according to flow cytometry (Fig. 1F). These results suggest that the isolated vesicles derived from the hUCMSCs met the criteria for exosomes, supporting subsequent investigations into their therapeutic potential.

scRNA-seq analysis of aging ovaries. To assess the expression profiles of PTEN and apoptosis-related molecules in aging ovaries, a scRNA-seq analysis was conducted. The scRNA-seq dataset (GSE130664) consisted of 2,601 single cells obtained from the ovaries of four young and four aged monkeys (34). The data were divided into two groups based on age (Old and Young group), allowing for the analysis of single cells from each group independently. The t-distributed stochastic neighbor embedding (t-SNE) method was utilized for dimensional reduction analysis (43). In the Old group, seven distinct cell types were identified, whilst the young monkey group contained eight cell types (Fig. S1A). Focus was primarily placed on oocytes and GCs for the present study. The key transcriptional regulators that modulate cell-type-specific gene regulatory networks, such as FIGLA for oocytes (44) and NR5A2 for GCs (45), are illustrated in t-SNE plots (Fig. S1B). To investigate the differences in PTEN and apoptotic protein expression between the two groups, a single-cell atlas displaying PTEN and caspase-3. The results revealed significantly the elevated expression of PTEN and caspase-3 in oocytes and GCs from the Old group compared with that in the Young group (Fig. S1C).

PTEN expression, apoptosis and proliferation in animal models of NOA. Animal experiments were subsequently conducted according to the design summarized in Fig. 2A. Briefly, exosome transplantation was performed twice in the Exos group, with a 7-day interval between each transplantation. After completing the treatment regimen, the mice from all three groups were sacrificed, and their ovaries and serum were collected for use in subsequent experiments. Prior to exosome transplantation, a comprehensive comparison of PTEN expression was conducted in the ovaries of the NOA and the Young groups, in addition to the extent of apoptosis and proliferation phenotypes. Western blot analysis and RT-qPCR were used to determine the levels of PTEN and apoptotic molecules, including Bax, Bcl-2, caspase-3 and caspase-9. The results of western blot analysis revealed elevated protein expression levels of PTEN, Bax, caspase-3 and caspase-9, but a reduced expression of Bcl-2 in the NOA group compared with the Young group (Fig. 2B). Similarly, the mRNA expression levels of PTEN, Bax, caspase-3 and caspase-9 were significantly increased in the NOA group, whilst the expression of Bcl-2 was notably decreased (Fig. 2C).

Additionally, TUNEL and EdU assays were performed on the ovarian sections to validate the significant differences in cellular apoptosis and proliferation found between the mice in the NOA group and the young mice. TUNEL assay revealed a notable increase in the apoptotic level of the ovaries of mice with NOA compared with that in the Young group (Fig. 2D). In addition, EdU assay revealed a significant reduction in ovarian cell proliferation in mice with NOA compared with those in the Young group (Fig. 2E). H&E staining of the ovarian tissues also revealed a marked decline in follicle numbers at all stages in mice with NOA compared with the young mice (Fig. 2F and G). Based on these findings, it was confirmed that the expression of PTEN and the level of apoptosis in the ovaries were increased, while the level of proliferation was decreased, in the aging ovaries of mice with NOA.

hUCMSC-Exos suppress apoptosis by negatively regulating PTEN expression in NOA mice. After completing the transplantation of hUCMSCs-Exos, the expression levels of PTEN and the degree of apoptosis and proliferation in the mouse ovarian tissue were explored to determine the therapeutic potential of exosomes. Specifically, western blot analysis and RT-qPCR were performed to assess the differences in the expression of PTEN and apoptosis-related molecules in the ovaries of the three groups. The results revealed that compared with the NOA group, the protein expression levels of PTEN and apoptosis-related molecules (Bax, caspase-3 and caspase-9) were decreased, while those of Bcl-2 were increased in the Exos group (Fig. 3A). Similarly, the mRNA expression levels of the aforementioned molecules exhibited a similar trend (Fig. 3B). These exosomal treatment outcomes suggest that Exos can inhibit PTEN, whilst suppressing apoptosis in the ovarian tissue in mice with NOA. TUNEL assay was then performed to further evaluate the extent of apoptosis in the ovarian tissue in the three groups, revealing a significant reversal of ovarian apoptosis in mice with NOA following treatment with hUCMSC-Exos (Fig. 3C).

Ovarian cell proliferation was then determined using EdU assay and immunostaining of proliferative-related molecules. EdU assay demonstrated a significant increase in proliferation in the ovarian tissues of mice with NOA following exosomal transplantation (Fig. 3D). Immunostaining for PCNA and Ki67, markers of cell proliferation, was performed to further measure the levels of proliferation in the three groups. Immunofluorescence staining of the ovarian sections revealed a marked increase in PCNA expression following exosomal transplantation compared with that in untreated mice with NOA (Fig. 4A). Similarly, the immunohistochemical and immunofluorescence staining of Ki67 revealed similar results. The expression of Ki67 in the ovaries of mice with NOA was found to be significantly increased after the MSC-derived exosome injection, indicating an improvement in the proliferation level (Fig. 4B and C). These experimental findings suggest that the transplantation of hUMSC-derived exosomes can effectively reduce the apoptosis of ovarian cells, whilst promoting ovarian cell proliferation, possibly by targeting PTEN.

hUCMSC-Exos treatment leads to the recovery of ovarian function in mice with NOA. To confirm the uptake of the injected exosomes by GCs *in vivo*, a tracing experiment was

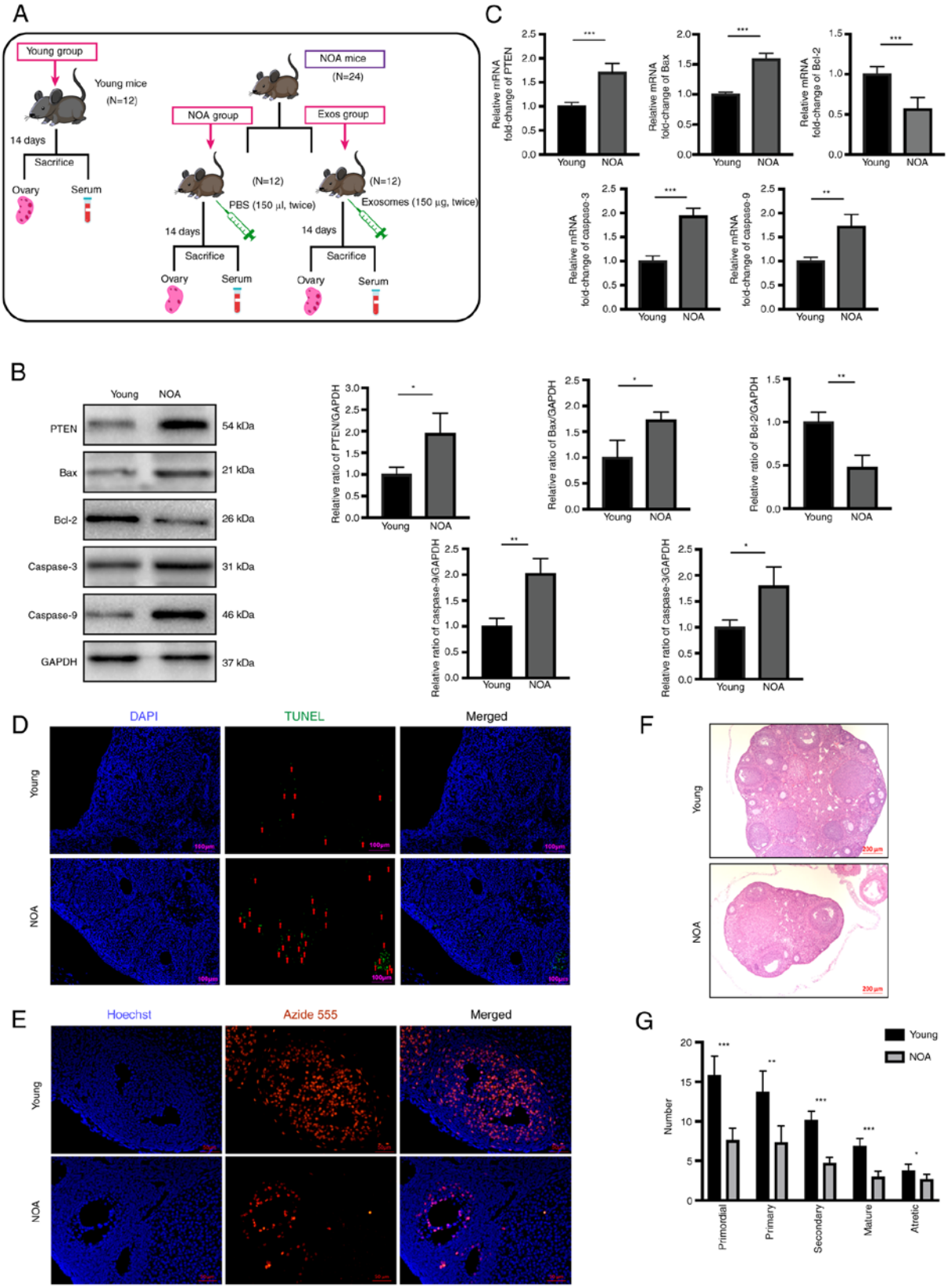

Figure 2. Apoptosis and proliferation levels in NOA. (A) Experimental timeline. Exosome transplantation was performed twice in the Exos group at 7-day intervals. At 2 weeks after treatment, mice from all three groups were sacrificed, and their ovaries and serum were collected for use in subsequent experiments. (B) Western blot analysis revealed the increased protein expression levels of PTEN, Bax, caspase-3 and caspase-9, and the decreased expression of Bcl-2 in ovarian tissues of the NOA group compared to the normal group. (C) Reverse transcription-quantitative PCR revealed significantly elevated mRNA levels of PTEN, Bax, caspase-3 and caspase-9, and the decreased expression of Bcl-2 in the ovarian tissues of the NOA group compared to the normal group. (D) TUNEL assay was performed to measure apoptosis of ovarian tissue in the NOA and normal groups. DAPI staining (blue fluorescence) indicates nuclei, while green fluorescence indicates apoptosis cells. Scale bars, 100 μm. (E) EdU assay was used to assess proliferation in the ovaries of the NOA and normal group. DAPI staining indicates nuclei, while red fluorescence indicates proliferating cells. Scale bars, 50 μm. (F) Hematoxylin and eosin staining of ovaries in the two different groups. Scale bars, 200 μm. (G) Follicle counts at various developmental stages between NOA and normal groups. Data are presented as the mean ± SD. *P<0.05, **P<0.01 and ***P<0.001, vs. young group. Data represent three independent experiments in each group. NOA, natural ovarian aging.

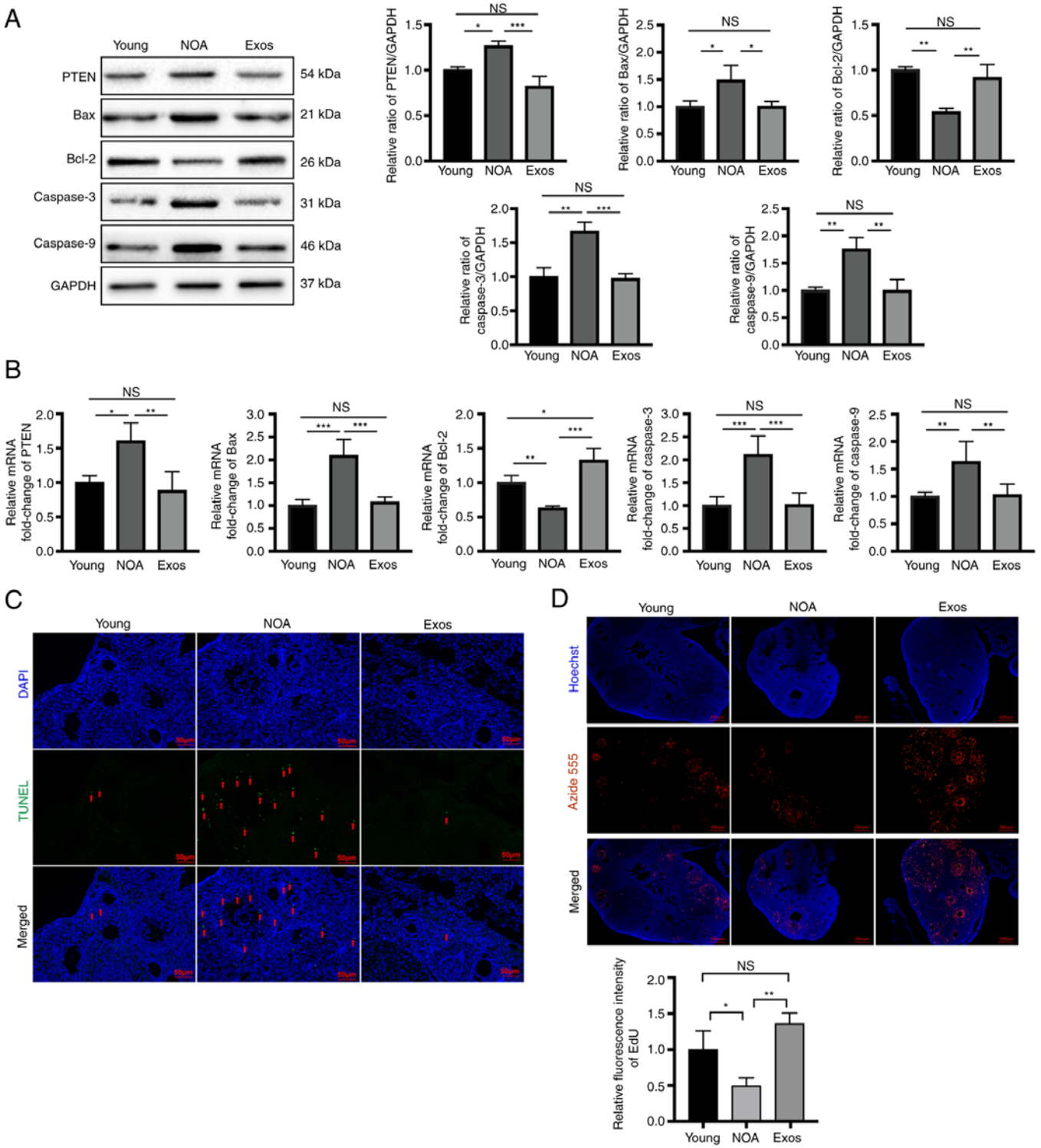

Figure 3. Exosomes suppress apoptosis and increase proliferation by negatively regulating PTEN expression in mice with NOA. (A) Following exosomal transplantation, western blot analysis revealed the decreased protein expression levels of PTEN, Bax, caspase-3 and caspase-9, and the increased expression of Bcl-2 in the ovarian tissues of the Exos group compared with the NOA group. (B) Following exosomal transplantation, reverse transcription-quantitative PCR revealed significantly reduced mRNA levels of PTEN, Bax, caspase-3 and caspase-9, and the elevated expression of Bcl-2 in ovarian tissues of the Exos group compared to the NOA group. (C) TUNEL assay was performed to measure apoptosis in the ovarian tissue in the three groups. DAPI staining (blue fluorescence) indicates nuclei, while green fluorescence indicates cells undergoing apoptosis. Scale bars, 50 μm. (D) EdU assay was used to assess proliferation in ovaries of the three different groups. DAPI staining indicates nuclei, while red fluorescence shows proliferating cells. Scale bars, 200 μm. Data are presented as the mean ± SD. *P<0.05, **P<0.01 and ***P<0.001; NS, not significant. Data represent three independent experiments in each group. NOA, natural ovarian aging; Exos, exosome-treated group.

conducted. The results revealed that after 5 days of exosome transplantation, the exosomes were taken up by the ovaries and internalized by the GCs, indicating their ability to infiltrate the ovarian cells (Fig. 5A). Subsequently, the status of ovarian function in the mice with NOA was evaluated. H&E-stained images of the ovarian tissue revealed that exosome delivery led to an increase in the number of follicles in all-stage and the restoration of follicular morphology within the ovary (Fig. 5B). To further assess the efficacy of hUCMSC-Exos in restoring ovarian aging, follicular numbers at different

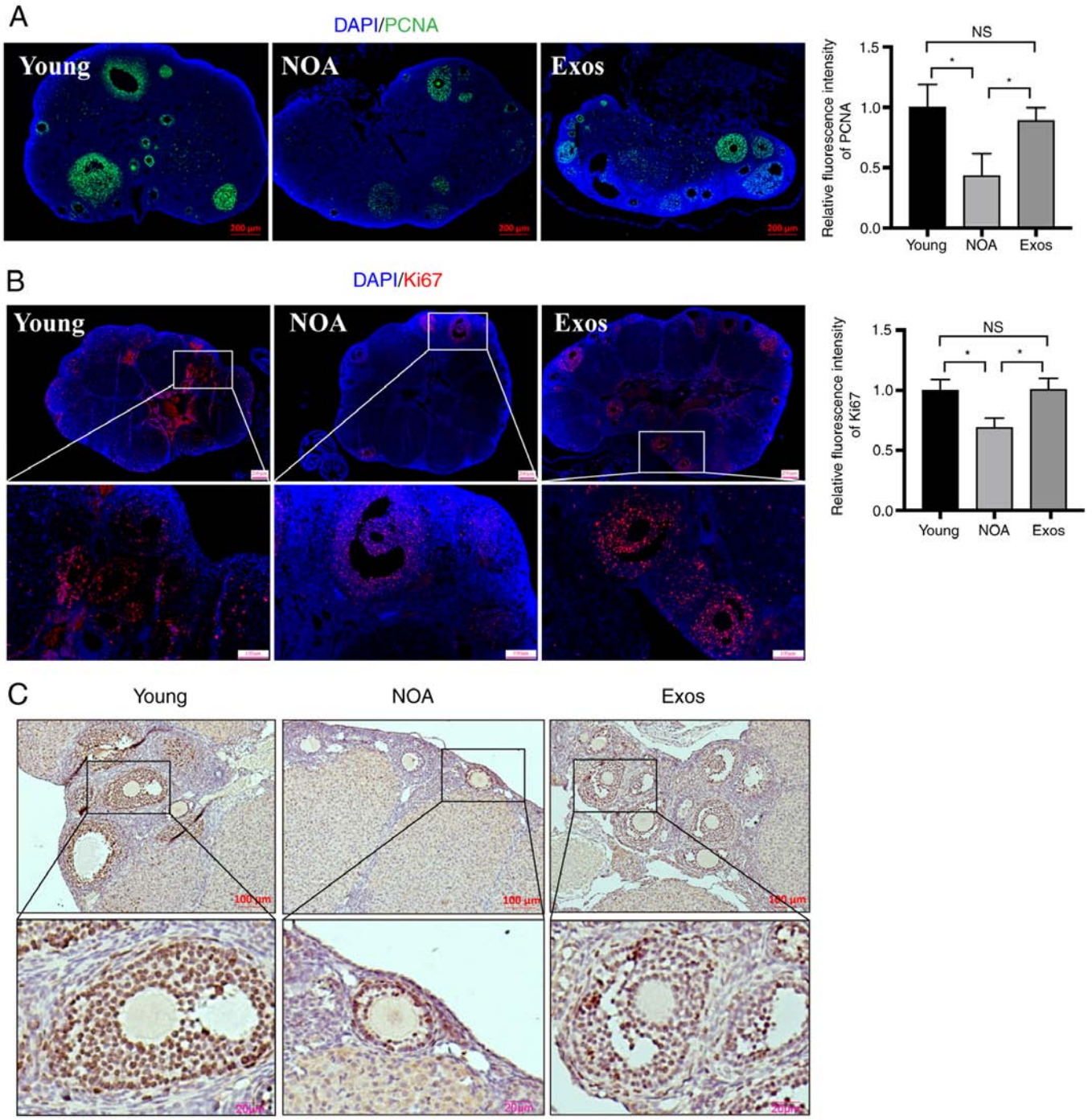

Figure 4. Exosomes enhance ovarian proliferation in mice with NOA. (A) Ovarian PCNA expression was assessed using immunofluorescence staining in the three groups. Scale bars, 200 μm. (B) Ovarian Ki67 expression was evaluated using immunohistochemical staining in the three groups. Scale bars, 100 and 200 μm. (C) Ovarian Ki67 expression was analyzed using immunofluorescence staining in the three groups. Scale bars, 200 and 50 μm. *P<0.05; NS, not significant. NOA, natural ovarian aging; Exos, exosome-treated group; PCNA, proliferating cell nuclear antigen.

stages were counted in ovarian tissues from mice in the three groups. It was observed that exosome transplantation led to a significant increase in the numbers of primordial, primary, secondary and mature follicles compared with the NOA group (Fig. 5C). The levels of AMH, E_2 and FSH in mouse serum were then measured using ELISA to evaluate the effectiveness of the exosomes in regulating the levels of reproductive hormones in mice with NOA. In the mice with NOA, the levels of AMH (Fig. 5D) and E_2 (Fig. 5E) were notably decreased, whilst those of FSH (Fig. 5F) were elevated, compared with those in the young mice. Following exosomal treatment, the levels of AMH (Fig. 5D) and E_2 (Fig. 5E) in the mice wotj NOA were increased, whereas those of FSH (Fig. 5F) were decreased. However, it should be noted that the AMH and FSH levels in the mice with NOA did not fully recover to the levels observed in the young mice following the completion of transplantation. These results suggest that exosomal transplantation can improve ovarian function in aging mice, although the complete restoration of hormone levels may not be achieved.

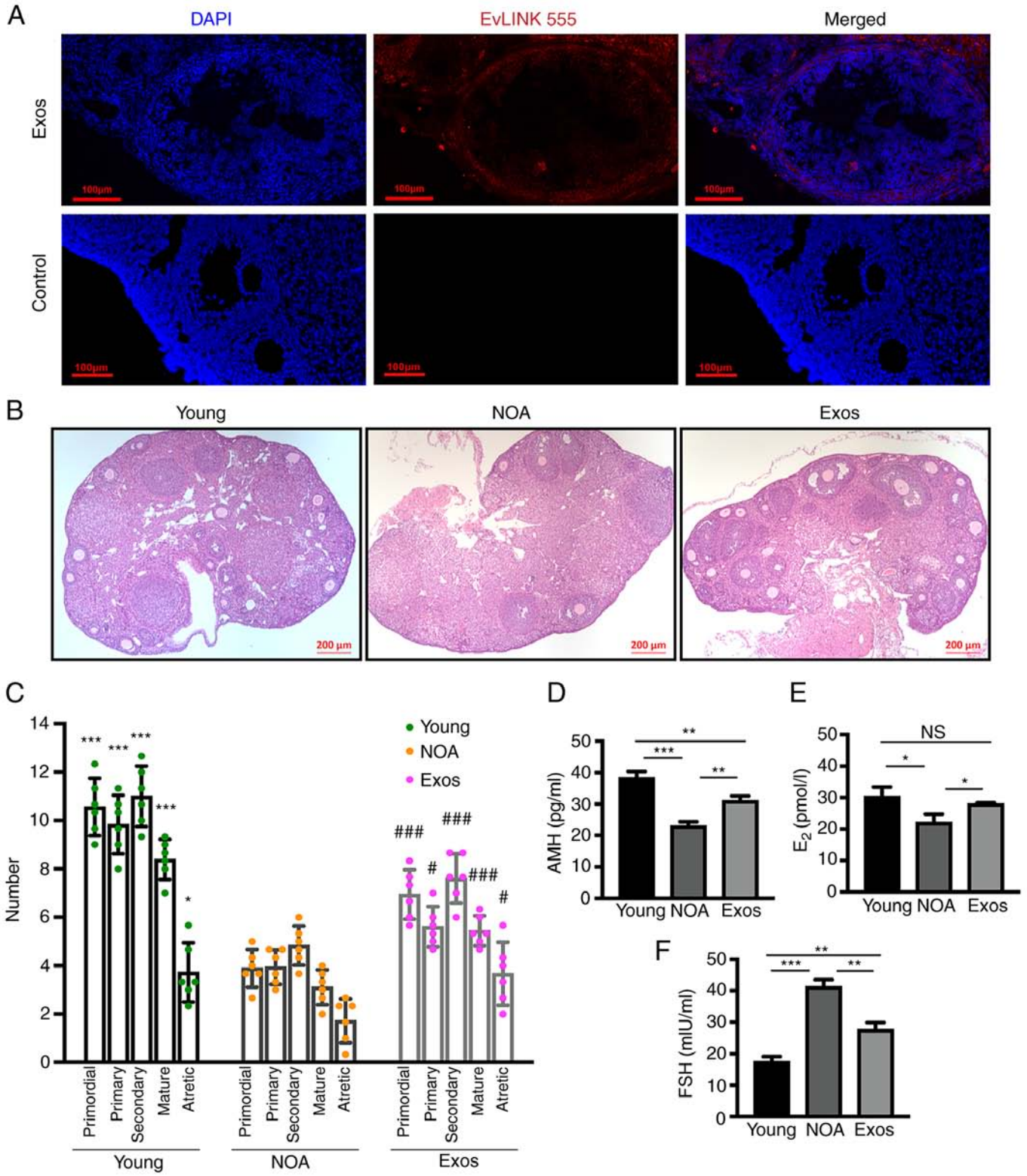

Figure 5. Exosomal treatment recovers ovarian function in mice with NOA. (A) Tracing experiment demonstrating uptake of injected exosomes by GCs *in vivo*. (B) Hematoxylin and eosin staining of ovaries in the three groups. Scale bars, 200 μm. (C) Quantification of follicles at different stages in each group. The presented statistical data represent the results of comparisons between the Young group and the Exo group with the NOA group. Levels of (D) AMH and (E) E_2 were significantly increased, while (F) the levels of FSH were decreased in the Exos group compared to the NOA group. Data are presented as the mean ± SD. *P<0.05, **P<0.01 and ***P<0.001, and $^{\#}$P<0.05 and $^{\#\#\#}$P<0.001 vs. NOA group; NS, not significant. Data represent three independent experiments in each group. NOA, natural ovarian aging; Exos, exosome-treated group; GCs, granulosa cells; AMH, anti-mullerian hormone; E2, estradiol; FSH, follicle stimulating hormone.

Identification of hGCs and establishment of the model of hGC apoptosis. To confirm the specific mechanisms underlying the effects of hUCMSC-Exos on apoptosis in NOA, the human ovarian granulosa cell line (HO-23) was used for establishing the cell model of apoptosis. The HO-23 cell line was established by transfection with simian virus 40 DNA, Ha-ras

oncogen, and a TS mutant of p53 (p53 Val135) (37,46). Under observation using a light microscope, the hGCs were observed to be polygonal or elliptical (Fig. S2A). Immunofluorescence staining revealed almost all of the cells were positive for FSHR expression in their cytoplasm, suggesting that this cell line was indeed ovarian GCs (Fig. S2B). Subsequently, Dil-labeled hUCMSCs-Exos were co-cultured with hGCs before Calcein-AM was used to stain the GCs. Through fluorescence imaging, the uptake of exosomes by hGCs was observed (Fig. S2C).

An apoptosis model of hGCs was then established by co-culturing the cells with CTX (CTX-hGCs). To verify the successful establishment of this cell apoptosis model, the expression of PTEN and apoptosis-related molecules were measured using western blot analysis and RT-qPCR. Moreover, the apoptotic and proliferative levels of hGCs were examined using TUNEL, CCK-8 and EdU assays. The protein and mRNA expression levels of PTEN and Bax were increased, whereas those of Bcl-2 were decreased (Fig. S2D and E). According to the findings of TUNEL assay, the apoptotic level of the CTX-treated GCs was notably increased compared with the untreated cells (Fig. S2F and G). Furthermore, from the results of CCK-8 assay, it was found that the proliferation of the CTX-GCs was markedly decreased compared with the untreated cells (Fig. S2H). The results from EdU assay also revealed that the quantity of proliferative cells markedly decreased following co-culture with CTX (Fig. S2I and J). These findings proved that the construction of the model of hGC apoptosis was successful.

hUCMSC-Exos inhibit the apoptosis of hGCs by regulating PTEN expression. After completing the establishment of the model of hGC apoptosis, hUCMSC-Exos were co-cultured with the cell model to assess the ability and mechanisms of the exosomes in preventing apoptosis. To investigate the specific role of PTEN-mediated apoptosis following exosomal treatment, western blot analysis and RT-qPCR were performed to detect the expression of PTEN and key molecules of apoptosis. Following treatment with exosomes, the expression levels of PTEN and pro-apoptotic molecules (Bax, caspase-3 and caspase-9) were markedly decreased, whereas the expression level of anti-apoptotic Bcl-2 was notably increased, according to the detection of protein and mRNA expression (Fig. 6A and B). Additionally, the apoptotic level of the GCs was assessed using TUNEL assay, whereas the proliferative level was evaluated using EdU and CCK-8 assays. Compared with the CTX-treated hGCs, the number of apoptotic hGCs, which were represented by green fluorescence in TUNEL assay, were found to be decreased following co-incubation of exosomes (Fig. 6C and D). In addition, the results of CCK-8 assay revealed that the proliferative level of GCs was markedly improved following co-culture with hUCMSC-Exos for 5 days compared with the CTX-treated hGCs (Fig. 6E). EdU assay of the three groups revealed there were more EdU-positive GCs following co-incubation with exosomes compared with the CTX group (Fig. 6F and G).

miR-21-5p is highly expressed in hUCMSC-Exos and is predicted to negatively regulate PTEN. miRNAs are one of the most critical functional molecules transported by exosomes that can exert regulatory inter-cellular effects. Herein, to further explore the specific molecules contained within hUCMSC-Exos that can target PTEN to inhibit apoptosis, sequencing of the miRNAs contained in the hUCMSC-Exos was conducted using high-throughput sequencing (Data S1). Bioinformatics analysis of these sequencing results was then performed. The heatmap of miRNAs revealed that miR-21-5p, miR-320a, miR-423-5p, miR-26a-5p and let-7g-5p were the five most highly expressed miRNAs in the hUCMSC-Exos (Fig. 7A). The individual molecular reads are presented in Fig. 7B. Furthermore, enrichment analysis of pathways activated by target genes of these top expressed miRNAs was then performed, based on the KEGG database (42). The PI3K/Akt pathway was found to be one of the significantly regulated pathways (Fig. 7C), with PTEN being one of the key regulators of this pathway (47). Through bioinformatics prediction and a review of the literature (48), miR-21-5p, the most highly expressed exosomal miRNA, was found to target and inhibit the expression of PTEN, which is a critical molecule that was verified by the aforementioned experiments to be significantly overexpressed in the ovaries in NOA and in the model of cell apoptosis. The potential seed sequence of miR-21-5p to the mRNA of PTEN is illustrated in Fig. 7D, where miR-21-5p was found to be highly conserved among species.

Exosomal miR-21-5p prevents GC apoptosis by negatively regulating PTEN expression. Following transfection with miR-21-5p mimics and inhibitor, the expression level of miR-21-5p in MSCs was significantly altered, with the mimics substantially increasing miR-21-5p expression (Fig. S3A), while the inhibitor decreased miR-21-5p expression (Fig. S3B). This confirmed the successful transfection and functional efficacy of miR-21-5p mimics/inhibitor. To verify the exosomal miRNA sequencing results, RT-qPCR was performed to evaluate the expression levels of miR-21-5p in the hUCMSC-Exos. The results revealed that miR-21-5p expression in the hUCMSC-Exos was significantly higher compared with that of miR-26a-5p (Fig. 8A). Following co-incubation with the hUCMSC-Exos, the hGCs were observed to take up the exosomes, where intracellular miR-21-5p expression increased (Fig. 8B). It was previously reported that miR-21-5p can repress PTEN expression (49). In addition, herein, miR-21-5p was found to be the most abundant molecule in the hUCMSC-Exos according to the high-throughput sequencing results. Therefore, it was hypothesized that exosome-derived miR-21-5p can target PTEN in the ovarian GCs of mice with NOA, thereby regulating their apoptotic and proliferative levels. To verify this targeting association, before the hUCMSC-Exos were used for co-culture with the CTX-treated hGCs, the inhibitor/mimics or inhibitor/mimics NC of miR-21-5p were transfected into the cells. Firstly, following transfection with inhibitor/mimics, miR-21-5p expression in the different groups was calculated using RT-qPCR after 48 h. Transfection with the inhibitor markedly inhibited miR-21-5p expression in the exosomes, whereas the mimics increased its expression following culture with the hGCs (miR-21-inhibtor/-mimics group vs. Exos group) (Fig. 8C). The results from RT-qPCR and western blot analysis revealed that following co-culture with the exosomes, PTEN expression in the cell model was notably suppressed compared with that in the untreated group

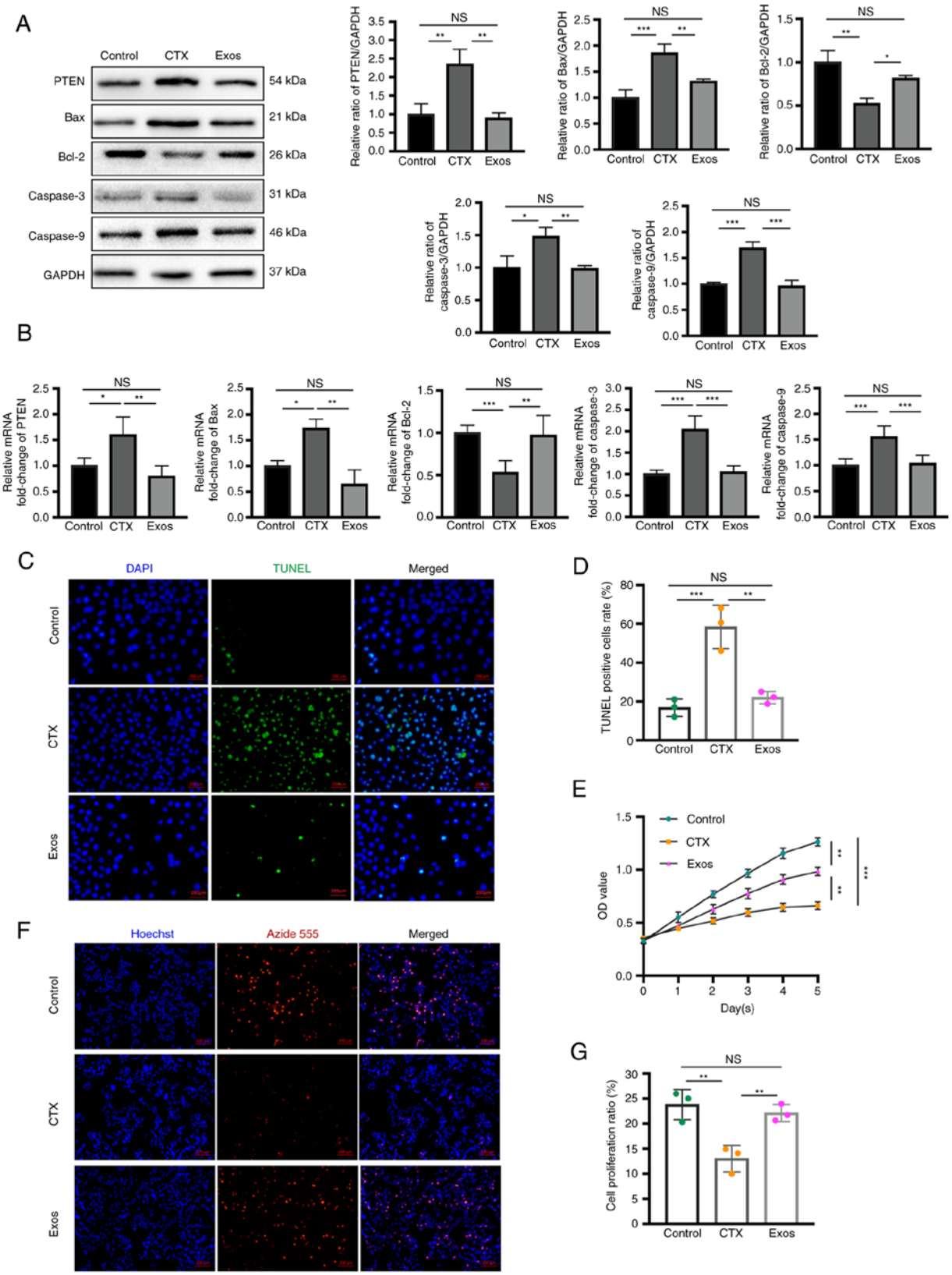

Figure 6. Exosomes suppress the apoptosis of CTX-treated hGCs by targeting PTEN. (A) Western blot analysis of hGCs revealed decreased protein expression of PTEN, Bax, caspase-3 and caspase-9, and increased the expression of Bcl-2 following co-culture with exosomes compared to the CTX group. (B) Reverse transcription-quantitative PCR demonstrated consistent expression trends of each molecule in hGCs among the three groups. (C) TUNEL assay reealed a significant reduction in apoptotic hGCs in the Exos group compared to CTX-treated hGCs. Scale bars, 200 μm. (D) The cellular apoptotic rate, calculated from TUNEL staining, was significantly higher in the Exos group than in the CTX group. (E) Viability of the hGCs was assessed using CCK-8 assay from days 0 to 5 in the three groups. (F) EdU assay demonstrated a marked increase in proliferating cells following co-culture of the CTX-treated hGCs with exosomes. DAPI stained the nucleus with blue fluorescence, and red fluorescence represented proliferating cells. Scale bars, 200 μm. (G) The cellular proliferation ratio, calculated from EdU staining, was significantly higher than in the Exos group compared to the CTX group. Data are presented as the mean ± SD. *P<0.05, **P<0.01 and ***P<0.001; NS, not significant. Data represent three independent experiments in each group. CTX, cyclophosphamide; hGCs, human granulosa cells; Exos, exosome-treated group.

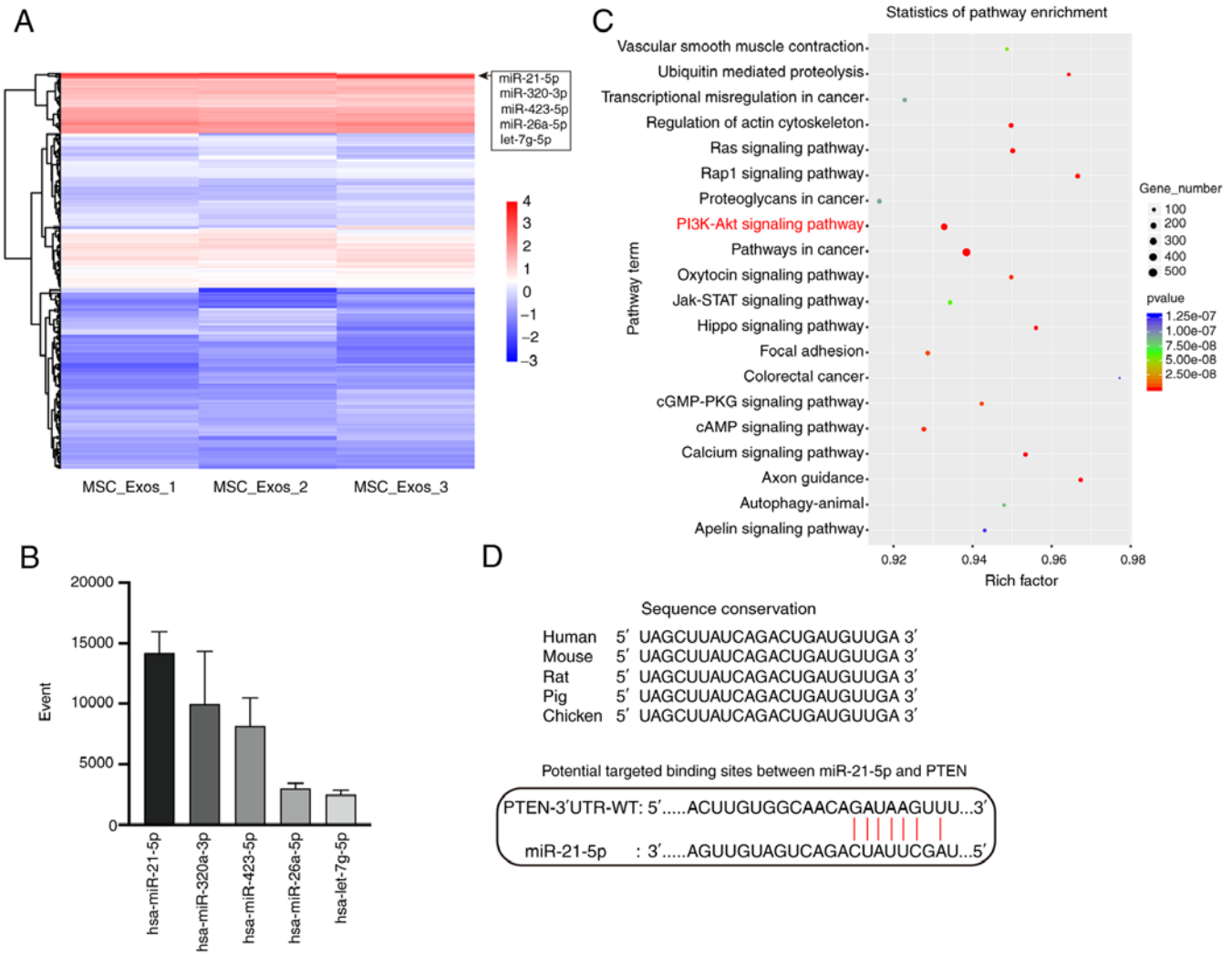

Figure 7. Exosomal miRNA sequencing and bioinformatics analysis results. (A) Heatmap displaying the expression profiles of miRNAs in exosomes from three samples, with five highly expressed miRNA molecules highlighted. (B) Individual molecular read counts of the five highly expressed miRNAs. (C) Kyoto Encyclopedia of Genes and Genomes analysis revealing the top enriched pathways regulated by the highly expressed exosomal miRNAs. (D) miR-21-5p is highly conserved among species, and bioinformatics analysis and references predicting the potential seed sequence of miR-21-5p binding to the mRNA of PTEN. Exos, exosomes.

(Fig. 8D and E). By contrast, this trend was reversed following transfection with miR-21-5p inhibitor. The protein expression of apoptosis-related molecules (Bax and Bcl-2) exhibited a corresponding trend, which was also reversed following miR-21-5p inhibitor transfection (Fig. 8E). Finally, miR-21-5p mimics were used to validate its contributions to the effects of hUCMSC-Exos treatment. The cells were either transfected with miRNA mimics or treated with exosomes. The results of western blot analysis demonstrated that transfection with mimics had the same effect as exosomal treatment, both of which were able to reduce PTEN expression and inhibit apoptosis (Fig. 8F).

Discussion

The findings of the present study strongly suggest the therapeutic potential of hUCMSC-derived exosomes in improving ovarian function in naturally aging ovaries. In addition, preliminarily investigations into the therapeutic mechanisms underlying this novel therapy were performed. Specifically, exosome-carried miRNAs regulate cell apoptosis by targeting PTEN, thereby exerting therapeutic functions (Figs. 2-8). Since aging is perceived to be a physiological process, it has received less attention compared with common 'diseases'. However, recent advancements in regenerative medicine have led to the proposal that aging is a treatable condition, with the slowing of the aging process emerging as a new frontier in medical development. In females, ovarian aging serves as the a catalyst and driver of senescence in other vital organs (50). Consequently, delaying ovarian aging provides a viable strategy with which to mitigate dysfunction and even age-related decline in other organs. Various approaches have been explored to combat ovarian aging, such as the use of antioxidants and promoting autophagy (51,52). However, the safety and efficacy of these methods remain controversial, impeding their practical clinical application. The aim of the present study was to enhance the current understanding of the underlying mechanisms of ovarian aging, and to propose and validate an effective method or concept that can partially or

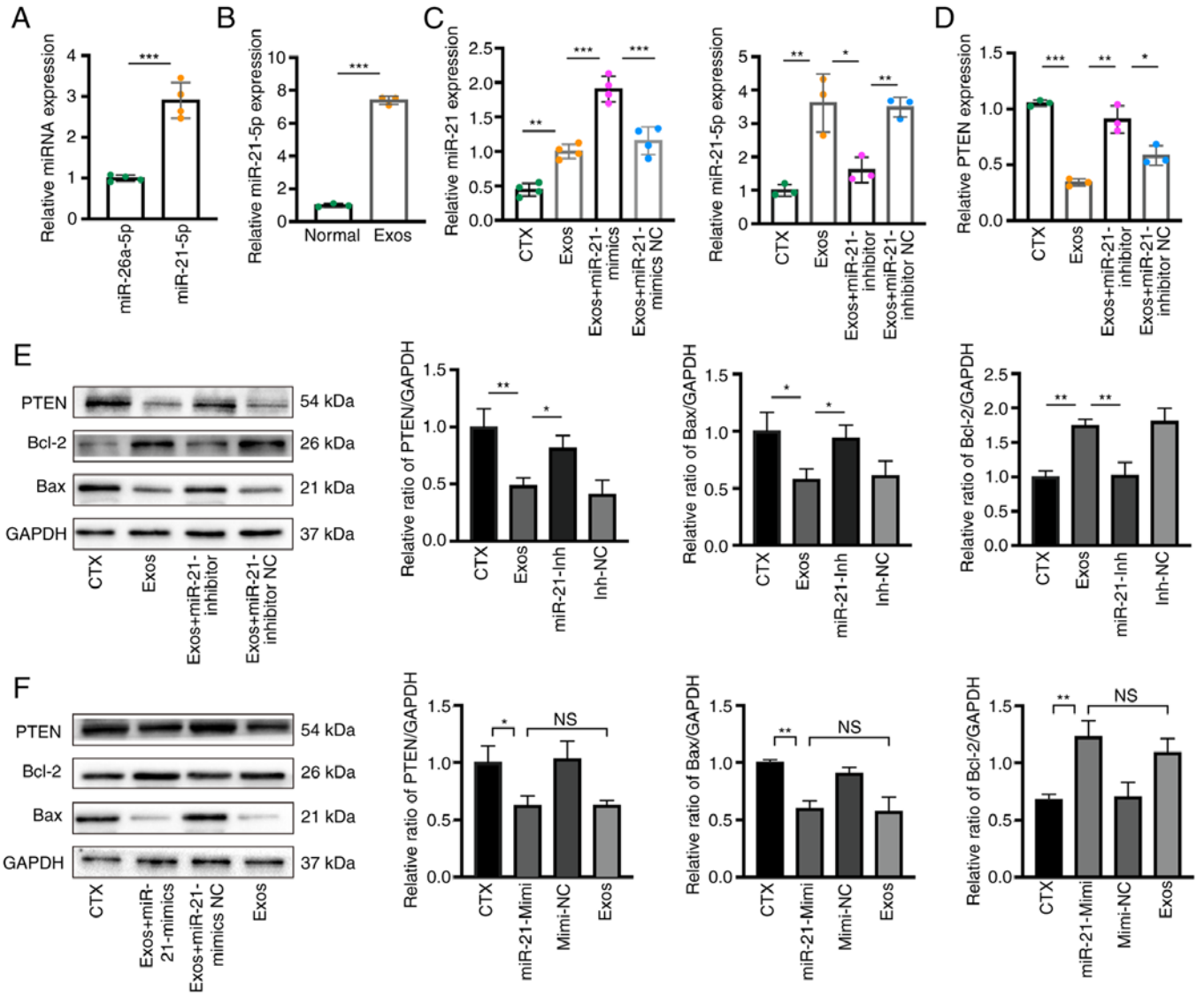

Figure 8. Exosomal miR-21-5p prevents hGC apoptosis by negatively regulating PTEN. (A) RT-qPCR assays revealed significantly higher levels of miR-21-5p in exosomes compared to miR-26a-5p. (B) RT-qPCR assays demonstrated the uptake of exosomes by hGCs and the increased intracellular levels of miR-21-5p. (C) RT-qPCR assays revealed that the miR-21-5p inhibitor significantly inhibited miR-21-5p expression in hGCs, while the mimics increased its level. (D) RT-qPCR results revealed the mRNA expression of PTEN in the four groups (the CTX group, Exos group, Exos + miR-21-inhibitor group, and Exos + miR-21-inhibitor NC). The inhibitory effect of exosomes on PTEN expression in hGCs was reversed by the miR-21-5p inhibitor. (E) Western blot analyses revealed the protein expression of PTEN, Bax, and Bcl-2 in the four groups. The effect of exosomes in inhibiting the PTEN expression and apoptotic level in hGCs was reversed by the miR-21-5p inhibitor. (F) Western blot analyses in the four groups (CTX group, Exos + miR-21-mimics group, Exos + miR-21-mimics NC group, and Exos group) demonstrated that the transfection of miR-21-5p mimics exerted the same inhibitory effect on PTEN and apoptosis levels as exosomal co-incubation. Data are presented as a percentage or mean ± SD; n=6 per group; *P<0.05, **P<0.01 and ***P<0.001; NS, not significant; hGCs, human granulosa cells; Exos, exosome-treated group; CTX, cyclophosphamide; RT-qPCR, reverse transcription-quantitative PCR.

fundamentally restore ovarian function. Exosomes derived from MSCs have emerged as a promising therapeutic approach for organ and tissue regeneration in various disorders, including decreased ovarian function (10,30). Therefore, in the present study, the effects of exosomes derived from hUCMSCs were examined in a mouse model of ovarian aging and in cell model (hGCs) of apoptosis. In addition, the present study explored the underlying mechanisms of MSC-derived exosomes in alleviating ovarian aging. These exosomes were found to exhibit the ability to partially restore the function of aging ovaries. Furthermore, the regulation of apoptosis by targeting PTEN through exosomal miR-21-5p may be a potential molecular mechanism of hUCMSC-Exos-mediated ovarian function recovery in NOA (Fig. 9).

Initially, a comprehensive analysis was conducted, which revealed a substantial increase in the apoptotic rate within the ovarian tissue of aged mice compared with that in young mice. Additionally, a noteworthy elevation in the expression levels of PTEN was found, a critical regulatory molecule of cellular apoptosis, in both natural aging mice and cell apoptosis models. These findings emphasize augmented apoptosis levels and upregulated PTEN expression as significant factors in the adverse effects of natural ovarian aging. PTEN has been frequently reported to be an oncogene that contributes to apoptosis induction in both cancerous and

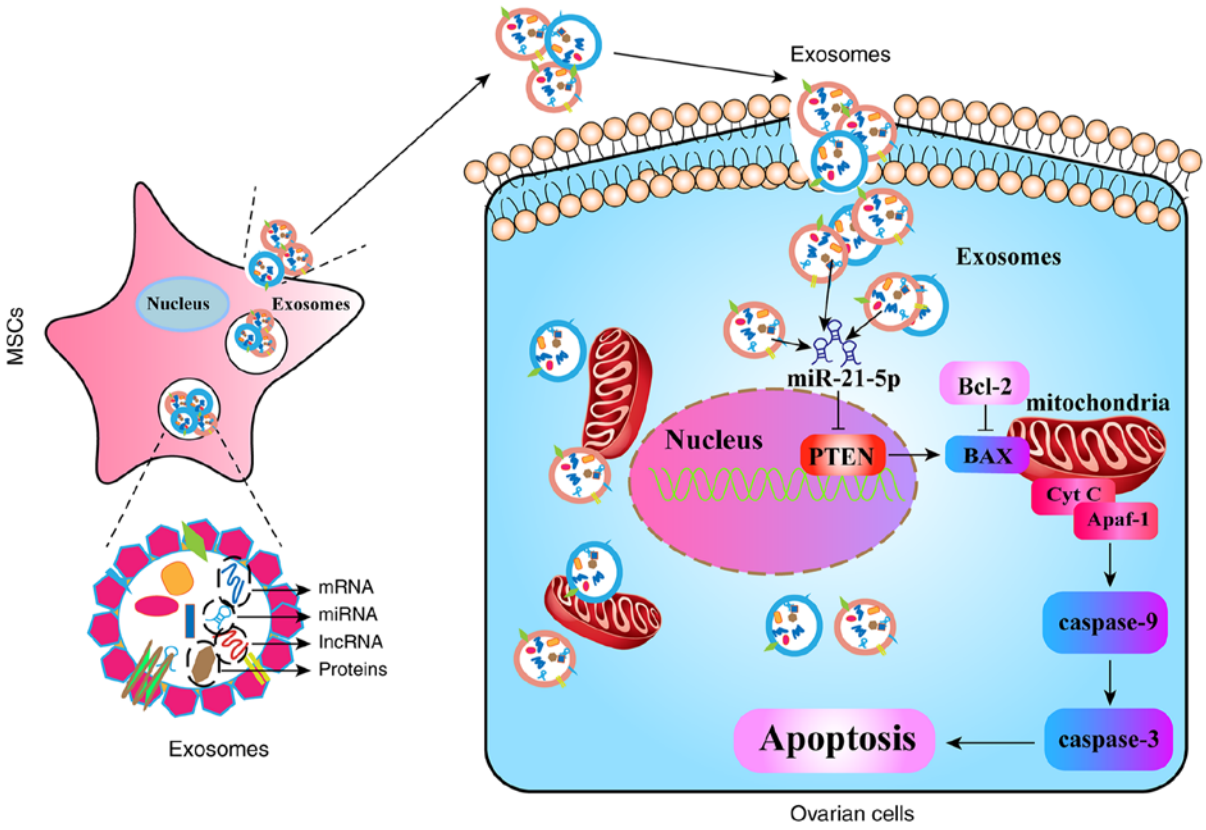

Figure 9. Schematic diagram illustrating the underlying therapeutic mechanisms of hUCMSC-Exos in addressing natural ovarian aging. Upon taken by ovarian cells, hUCMSC-Exos deliver miR-21-5p, which targets and suppresses the expression of PTEN. This inhibition of PTEN leads to the attenuation of the downstream apoptotic pathway, ultimately resulting in reduced cellular apoptosis. hUCMSCs, human umbilical cord-derived mesenchymal stem cells; hUCMSC-Exos, hUCMSC-derived exosomes.

normal cells (53). Its essential role in various physiological and pathological processes is evident through its regulation of apoptotic degrees in different tissues and organs (54). Through its modulation of the AKT phosphorylation level, PTEN exerts control over numerous cellular, including cellular viability, proliferation and apoptosis (55). Notably, the PTEN-PI3K/AKT pathway has been reported to play a crucial role in the activation of primordial follicular and the process of ovarian aging (56). In the present study, following exosomal treatment, a significant decrease in PTEN expression was found in both aging ovaries and cellular models. Therefore, it was hypothesized that the exosomes contain specific miRNA molecules capable of targeting and regulating PTEN, thereby exerting downstream functions. Therefore, the modulation of PTEN expression and function was likely to be a vital mechanism through which hUCMSC-derived exosomes can regulate apoptosis in aged ovaries.

Even though a number of studies focusing on the therapeutic effects of MSC-Exos have been performed, the inherent therapeutic mechanisms and the molecular components of MSC-derived exosomes have been poorly elucidated. Exosomes are generally 30-150 nm in size and are lipidic micro-vesicles. They are typically secreted by cells into the extracellular environment (57). These vesicles selectively incorporate particular non-coding RNAs, allowing for intercellular communication by through exosomal transport between neighboring cells. Through this mechanism, exosomes can potentially play crucial roles in regulating physiological processes and disease progression. Among the various components of exosomes, miRNAs are particularly important for their biological functions, as they can modulate ~50% of the gene expression and function in the human body (58). miRNAs are highly abundant in MSCs-Exos and possess regulatory properties in target-damaged organs, by suppressing the translation and activation of target genes by binding to the 3'-UTR of their corresponding mRNAs (59-61). Against ovarian dysfunction, miRNAs derived from MSC-Exos have been documented to play a vital role in restoring ovarian function through multiple mechanisms, including promoting proliferation and inhibiting apoptosis (62). While some studies have utilized MSC-Exos to address premature ovarian insufficiency (10,29), only a limited number of studies have explored the potential of these for restoring ovarian function in naturally aging ovaries (30). A previous study achieved satisfactory results in managing NOA using human amniotic MSCs (30). However, that study only provided a basic exploration of the therapeutic mechanism and did not utilize MSC-derived exosomes (30). Therefore, the present study was performed to assess the effects of MSC-derived exosomes by administering them to naturally aged ovaries and investigated the underlying mechanisms at the molecular regulatory level.

To elucidate the molecular mechanisms underlying exosome-mediated treatment and examine the effects of hUCMSC-Exos on PTEN expression, miRNA sequencing of hUCMSCs-Exos was performed before the results were

screened for the most abundant miRNA molecules that can target PTEN. This precise sequencing method of exosomal miRNAs was used to avoid ambiguity. High-throughput sequencing and laboratory experiments revealed that miR-21-5p was abundantly expressed in the hUCMSC-Exos. Previous studies have reported the ability of miR-21 to modulate the expression and function of intracellular PTEN, establishing PTEN as a downstream target of miR-21 (48,49,63). Consequently, the present study focused on investigating the linear regulatory association between exosomal miR-21, PTEN and apoptosis. Bioinformatics analysis further demonstrated that miR-21-5p effectively regulated and inhibit the function of PTEN molecules. Subsequent experiments confirmed that the increased expression of miR-21-5p and the decreased expression of PTEN in GCs were attributed to the cellular uptake of exosomes. Notably, the positive results of exosomes in targeting PTEN and inhibiting apoptosis were reversed by transfection with miR-21-5p inhibitor, while transfection with miR-21-5p mimics alone also effectively suppressed the onset of apoptosis. These findings suggest that miR-21-5p contained within hUCMSC-derived exosomes targets PTEN to prevent apoptosis, highlighting its role in the molecular mechanisms underlying the effects mediated by exosomal treatment for NOA.

The ability of MSC-derived exosomes to regulate the expression of genes associated with ovarian aging renders them a highly promising therapeutic strategy for alleviating natural ovarian dysfunction. In comparison with previous research (30), the present study utilized MSC-derived exosomes and employed high-throughput miRNA sequencing, which enabled investigations into their molecular mechanisms with precision. Consequently, the present study showcases notable innovations in the field of MSC-derived exosomal therapy for ovarian aging. The positive outcomes hold significant value in establishing the theoretical framework for MSC- and MSC-Exos-mediated therapy, laying a solid foundation for future clinical applications. In the future, targeted therapy based on specialized miRNA may emerge as a promising avenue to combat and slow down ovarian aging.

Despite the encouraging results obtained in this study, there are several limitations that should be acknowledged, and further work is necessary. The route, dose, and frequency of exosomal transplantation were tentatively determined based on preliminary experiments and previous studies. Standardization of these parameters is crucial before clinical application to ensure its effectiveness and consistency. In addition, since fertility restoration is not the primary focus in naturally aging individuals, the fertility status of the NOA model was not evaluated. Due to concerns regarding the potential adverse effects of anesthesia and the technical challenges associated with collecting blood samples from live mice, serum was not collected from the same mice before and 14 days following exosome transplantation *in vivo* in the present study. Future studies are required to systematically establish the criteria and protocols for exosome administration, utilizing *in vivo* and *in vitro* experiments to thoroughly evaluate their therapeutic efficacy. Additionally, inflammatory factors were not specifically investigated to assess the contributions of immune reactions in this cross-species transplantation study. Subsequent research is required to include the detection of immune indicators to confirm the safety of cross-species transplantation of MSC-exos. The present study also did not investigate the effects of various concentration gradients of exosomal transplantation. Thus, further studies are warranted to determine the dose gradient to be used as a core parameter to further strengthen the validity and reliability of the present findings.

In conclusion, the present study provides evidence that exosomes derived from hUCMSCs have the ability to enhance the function of naturally aging ovaries. The underlying molecular mechanisms involve the regulation of cellular apoptosis through the inhibition of PTEN expression by exosomal miR-21-5p in ovarian cells. The positive experimental results strongly support the potential of hUCMSC-Exos transplantation as a promising therapy for improving ovarian function in the context of natural aging.

Acknowledgements

Not applicable.

Funding

The present study was financially supported by the Excellent Clinical Medicine Talent Training Project funded by the Hebei Provincial Government in 2022 (funding project title: 'Umbilical cord mesenchymal stem cell-derived exosomes regulate the level of epigenetic modification to restore ovarian function'.

Availability of data and materials

The datasets used and/or analyzed during the current study are available from the corresponding author on reasonable request.

Authors' contributions

ZL, YL, YD, JZ and XH conceived and designed the study. ZL, YL, YaT and QL conducted the experiments and wrote the manuscript. HZ, SY and YiT were responsible for the identification of the mesenchymal stem cells and exosomes. YD, WS and TY were responsible for data analysis and for figure preparation/creation. WS, YaT and XH discussed and revised the manuscript. XH and ZL reviewed the manuscript. All authors have read and approved the final manuscript. ZL and YD confirm the authenticity of all the raw data.

Ethics approval and consent to participate

The principles outlined in the Declaration of Helsinki and the Guidelines for the Care and Use of Laboratory Animals of the Chinese Institute of Health were strictly adhered to in the present study. The authors also complied with the ARRIVE guidelines. Ethical approval for the animal experiments was obtained from the Ethical Committee of Second Hospital of Hebei Medical University (approval no. 2021-AE034). All animal experiments conducted in the present study followed the guidelines and regulations specified in this ethical approval.

Patient consent for publication

Not applicable.

Competing interests

The authors HZ, SY and YiT were affiliated with Qilu Cell Therapy Technology Co., Ltd. The remaining authors affirm that the research was conducted without any commercial or financial associations that may be perceived as a potential conflict of interest.

References

1. Edson MA, Nagaraja AK and Matzuk MM: The mammalian ovary from genesis to revelation. Endocr Rev 30: 624-712, 2009.
2. Nelson SM, Telfer EE and Anderson RA: The ageing ovary and uterus: New biological insights. Hum Reprod Update 19: 67-83, 2013.
3. Broekmans FJ, Soules MR and Fauser BC: Ovarian aging: Mechanisms and clinical consequences. Endocr Rev 30: 465-493, 2009.
4. Park SU, Walsh L and Berkowitz KM: Mechanisms of ovarian aging. Reproduction 162: R19-R33, 2021.
5. Lew R: Natural history of ovarian function including assessment of ovarian reserve and premature ovarian failure. Best Pract Res Clin Obstet Gynaecol 55: 2-13, 2019.
6. Chon SJ, Umair Z and Yoon MS: Premature ovarian insufficiency: Past, present, and future. Front Cell Dev Biol 9: 672890, 2021.
7. Seli E: Ovarian aging. Semin Reprod Med 33: 375-376, 2015.
8. Check Hayden E: Anti-ageing pill pushed as bona fide drug. Nature 522: 265-266, 2015.
9. Sullivan SD, Sarrel PM and Nelson LM: Hormone replacement therapy in young women with primary ovarian insufficiency and early menopause. Fertility Sterility 106: 1588-1599, 2016.
10. Ding C, Zhu L, Shen H, Lu J, Zou Q, Huang C, Li H and Huang B: Exosomal miRNA-17-5p derived from human umbilical cord mesenchymal stem cells improves ovarian function in premature ovarian insufficiency by regulating SIRT7. Stem Cells 38: 1137-1148, 2020.
11. Pittenger MF, Mackay AM, Beck SC, Jaiswal RK, Douglas R, Mosca JD, Moorman MA, Simonetti DW, Craig S and Marshak DR: Multilineage potential of adult human mesenchymal stem cells. Science 284: 143-147, 1999.
12. Yin N, Wu C, Qiu J, Zhang Y, Bo L, Xu Y, Shi M, Zhu S, Yang G and Mao C: Protective properties of heme oxygenase-1 expressed in umbilical cord mesenchymal stem cells help restore the ovarian function of premature ovarian failure mice through activating the JNK/Bcl-2 signal pathway-regulated autophagy and upregulating the circulating of $CD8^{+}CD28^{-}$ T cells. Stem Cell Res Ther 11: 49, 2020.
13. Martinez-Carrasco R, Sanchez-Abarca LI, Nieto-Gomez C, Martin Garcia E, Sanchez-Guijo F, Argueso P, Aijón J, Hernández-Galilea E and Velasco A: Subconjunctival injection of mesenchymal stromal cells protects the cornea in an experimental model of GVHD. Ocul Surf 17: 285-294, 2019.
14. Oliva J: Therapeutic properties of mesenchymal stem cell on organ ischemia-reperfusion injury. Int J Mol Sci 20: 5511, 2019.
15. Salado-Manzano C, Perpina U, Straccia M, Molina-Ruiz FJ, Cozzi E, Rosser AE and Canals JM: Is the immunological response a bottleneck for cell therapy in neurodegenerative diseases? Front Cell Neurosci 14: 250, 2020.
16. Sajeesh S, Broekelman T, Mecham RP and Ramamurthi A: Stem cell derived extracellular vesicles for vascular elastic matrix regenerative repair. Acta Biomater 113: 267-278, 2020.
17. Ranganath SH, Levy O, Inamdar MS and Karp JM: Harnessing the mesenchymal stem cell secretome for the treatment of cardiovascular disease. Cell Stem Cell 10: 244-258, 2012.
18. Valadi H, Ekstrom K, Bossios A, Sjostrand M, Lee JJ and Lotvall JO: Exosome-mediated transfer of mRNAs and microRNAs is a novel mechanism of genetic exchange between cells. Nat Cell Biol 9: 654-659, 2007.
19. Kalluri R and LeBleu VS: The biology, function, and biomedical applications of exosomes. Science 367L: eaau6977, 2020.
20. Yao J, Ma Y, Zhou S, Bao T, Mi Y, Zeng W, Li J and Zhang C: Metformin prevents follicular atresia in aging laying chickens through activation of PI3K/AKT and calcium signaling pathways. Oxid Med Cell Longev 2020: 3648040, 2020.
21. Tilly JL, Kowalski KI, Johnson AL and Hsueh AJ: Involvement of apoptosis in ovarian follicular atresia and postovulatory regression. Endocrinology 129: 2799-2801, 1991.
22. Shen M, Lin F, Zhang J, Tang Y, Chen WK and Liu H: Involvement of the up-regulated FoxO1 expression in follicular granulosa cell apoptosis induced by oxidative stress. J Biol Chem 287: 25727-25740, 2012.
23. Matsuda F, Inoue N, Manabe N and Ohkura S: Follicular growth and atresia in mammalian ovaries: Regulation by survival and death of granulosa cells. J Reprod Dev 58: 44-50, 2012.
24. Yamada KM and Araki M: Tumor suppressor PTEN: Modulator of cell signaling, growth, migration and apoptosis. J Cell Sci 114: 2375-2382, 2001.
25. Stambolic V, Suzuki A, de la Pompa JL, Brothers GM, Mirtsos C, Sasaki T, Ruland J, Penninger JM, Siderovski DP and Mak TW: Negative regulation of PKB/Akt-dependent cell survival by the tumor suppressor PTEN. Cell 95: 29-39, 1998.
26. Maidarti M, Anderson RA and Telfer EE: Crosstalk between PTEN/PI3K/Akt signalling and DNA damage in the oocyte: Implications for primordial follicle activation, oocyte quality and ageing. Cells 9: 200, 2020.
27. Hsueh AJ, Kawamura K, Cheng Y and Fauser BC: Intraovarian control of early folliculogenesis. Endocr Rev 36: 1-24, 2015.
28. Wen Z, Mai Z, Zhu X, Wu T, Chen Y, Geng D and Wang J: Mesenchymal stem cell-derived exosomes ameliorate cardiomyocyte apoptosis in hypoxic conditions through microRNA144 by targeting the PTEN/AKT pathway. Stem Cell Res Ther 11: 36, 2020.
29. Ding C, Qian C, Hou S, Lu J, Zou Q, Li H and Huang B: Exosomal miRNA-320a is released from hAMSCs and regulates SIRT4 to prevent reactive oxygen species generation in POI. Mol Ther Nucleic Acids 21: 37-50, 2020.
30. Ding C, Zou Q, Wang F, Wu H, Chen R, Lv J, Ling M, Sun J, Wang W, Li H and Huang B: Human amniotic mesenchymal stem cells improve ovarian function in natural aging through secreting hepatocyte growth factor and epidermal growth factor. Stem Cell Res Ther 9: 55, 2018.
31. Dominici M, Le Blanc K, Mueller I, Slaper-Cortenbach I, Marini F, Krause D, Deans R, Keating A, Prockop DJ and Horwitz E: Minimal criteria for defining multipotent mesenchymal stromal cells. The International Society for Cellular Therapy position statement. Cytotherapy 8: 315-357, 2006.
32. Li Z, Zhang M, Zheng J, Tian Y, Zhang H, Tan Y, Li Q, Zhang J and Huang X: Human umbilical cord mesenchymal stem Cell-derived exosomes improve ovarian function and proliferation of premature ovarian insufficiency by regulating the hippo signaling pathway. Front Endocrinol (Lausanne) 12: 711902, 2021.
33. Lotvall J, Hill AF, Hochberg F, Buzas EI, Di Vizio D, Gardiner C, Gho YS, Kurochkin IV, Mathivanan S, Quesenberry P, *et al*: Minimal experimental requirements for definition of extracellular vesicles and their functions: A position statement from the international society for extracellular vesicles. J Extracell Vesicles 3: 26913, 2014.
34. Wang S, Zheng Y, Li J, Yu Y, Zhang W, Song M, Liu Z, Min Z, Hu H, Jing Y, *et al*: Single-cell transcriptomic atlas of primate ovarian aging. Cell 180: 585-600.e19, 2020.
35. Zhang X, Lan Y, Xu J, Quan F, Zhao E, Deng C, Luo T, Xu L, Liao G, Yan M, *et al*: CellMarker: A manually curated resource of cell markers in human and mouse. Nucleic Acids Res 47: D721-D728, 2019.
36. Liu M, Qiu Y, Xue Z, Wu R, Li J, Niu X, Yuan J, Wang Y and Wu Q: Small extracellular vesicles derived from embryonic stem cells restore ovarian function of premature ovarian failure through PI3K/AKT signaling pathway. Stem Cell Res Ther 11: 3, 2020.
37. Hosokawa K, Dantes A, Schere-Levy C, Barash A, Yoshida Y, Kotsuji F, Vlodavsky I and Amsterdam A: Induction of Ad4BP/SF-1, steroidogenic acute regulatory protein, and cytochrome P450scc enzyme system expression in newly established human granulosa cell lines. Endocrinology 139: 4679-4687, 1998.
38. Havelock JC, Rainey WE and Carr BR: Ovarian granulosa cell lines. Mol Cell Endocrinol 228: 67-78, 2004.
39. Livak KJ and Schmittgen TD: Analysis of relative gene expression data using real-time quantitative PCR and the 2(-Delta Delta C(T)) method. Methods 25: 402-408, 2001.

40. Salic A and Mitchison TJ: A chemical method for fast and sensitive detection of DNA synthesis in vivo. Proc Natl Acad Sci USA 105: 2415-2420, 2008.
41. Park CM, Reid PE, Walker DC and MacPherson BR: A simple, practical 'swiss roll' method of preparing tissues for paraffin or methacrylate embedding. J Microsc 145: 115-120, 1987.
42. Kanehisa M and Goto S: KEGG: Kyoto encyclopedia of genes and genomes. Nucleic Acids Res 28: 27-30, 2000.
43. Lake BB, Ai R, Kaeser GE, Salathia NS, Yung YC, Liu R, Wildberg A, Gao D, Fung HL, Chen S, *et al*: Neuronal subtypes and diversity revealed by single-nucleus RNA sequencing of the human brain. Science 352: 1586-1590, 2016.
44. Soyal SM, Amleh A and Dean J: FIGalpha, a germ cell-specific transcription factor required for ovarian follicle formation. Development 127: 4645-4654, 2000.
45. Meinsohn MC, Morin F, Bertolin K, Duggavathi R, Schoonjans K and Murphy BD: The orphan nuclear receptor liver homolog Receptor-1 (Nr5a2) regulates ovarian granulosa cell proliferation. J Endocr Soc 2: 24-41, 2018.
46. Sasson R, Tajima K and Amsterdam A: Glucocorticoids protect against apoptosis induced by serum deprivation, cyclic adenosine 3',5'-monophosphate and p53 activation in immortalized human granulosa cells: Involvement of Bcl-2. Endocrinology 142: 802-811, 2001.
47. Carracedo A and Pandolfi PP: The PTEN-PI3K pathway: Of feedbacks and cross-talks. Oncogene 27: 5527-5541, 2008.
48. Meng F, Henson R, Wehbe-Janek H, Ghoshal K, Jacob ST and Patel T: MicroRNA-21 regulates expression of the PTEN tumor suppressor gene in human hepatocellular cancer. Gastroenterology 133: 647-658, 2007.
49. Zhang JG, Wang JJ, Zhao F, Liu Q, Jiang K and Yang GH: MicroRNA-21 (miR-21) represses tumor suppressor PTEN and promotes growth and invasion in non-small cell lung cancer (NSCLC). Clin Chim Acta 411: 846-852, 2010.
50. Zhang J, Chen Q, Du D, Wu T, Wen J, Wu M, Zhang Y, Yan W, Zhou S, Li Y, *et al*: Can ovarian aging be delayed by pharmacological strategies? Aging (Albany NY) 11: 817-832, 2019.
51. Sugiyama M, Kawahara-Miki R, Kawana H, Shirasuna K, Kuwayama T and Iwata H: Resveratrol-induced mitochondrial synthesis and autophagy in oocytes derived from early antral follicles of aged cows. J Reprod Dev 61: 251-259, 2015.
52. Yan F, Zhao Q, Li Y, Zheng Z, Kong X, Shu C, Liu Y and Shi Y: The role of oxidative stress in ovarian aging: A review. J Ovarian Res 15: 100, 2022.
53. Weng LP, Smith WM, Dahia PL, Ziebold U, Gil E, Lees JA and Eng C: PTEN suppresses breast cancer cell growth by phosphatase activity-dependent G1 arrest followed by cell death. Cancer Res 59: 5808-5814, 1999.
54. Huang H, Potter CJ, Tao W, Li DM, Brogiolo W, Hafen E, Sun H and Xu T: PTEN affects cell size, cell proliferation and apoptosis during Drosophila eye development. Development 126: 5365-5372, 1999.
55. Song MS, Salmena L and Pandolfi PP: The functions and regulation of the PTEN tumour suppressor. Nat Rev Mol Cell Biol 13: 283-296, 2012.
56. Llarena N and Hine C: Reproductive longevity and aging: Geroscience approaches to maintain long-term ovarian fitness. J Gerontol A Biol Sci Med Sci 76: 1551-1560, 2021.
57. Ferguson SW and Nguyen J: Exosomes as therapeutics: The implications of molecular composition and exosomal heterogeneity. J Control Release 228: 179-190, 2016.
58. Lu J and Clark AG: Impact of microRNA regulation on variation in human gene expression. Genome Res 22: 1243-1254, 2012.
59. Bushati N and Cohen SM: microRNA functions. Annu Rev Cell Dev Biol 23: 175-205, 2007.
60. Ferguson SW, Wang J, Lee CJ, Liu M, Neelamegham S, Canty JM and Nguyen J: The microRNA regulatory landscape of MSC-derived exosomes: A systems view. Sci Rep 8: 1419, 2018.
61. Cai Y, Yu X, Hu S and Yu J: A brief review on the mechanisms of miRNA regulation. Genomics Proteomics Bioinformatics 7: 147-154, 2009.
62. Yang M, Lin L, Sha C, Li T, Zhao D, Wei H, Chen Q, Liu Y, Chen X, Xu W, *et al*: Bone marrow mesenchymal stem cell-derived exosomal miR-144-5p improves rat ovarian function after chemotherapy-induced ovarian failure by targeting PTEN. Lab Invest 100: 342-352, 2020.
63. Fu X, He Y, Wang X, Peng D, Chen X, Li X and Wang Q: Overexpression of miR-21 in stem cells improves ovarian structure and function in rats with chemotherapy-induced ovarian damage by targeting PDCD4 and PTEN to inhibit granulosa cell apoptosis. Stem Cell Res Ther 8: 187, 2017.